David Ortega [1], Carles Roqué [2], Jordi Ibáñez [3], Elisabet Beamud [4], Juan C. Larrasoaña [4,5], Alberto Sáez [6], Xavier Terradas [1 (*)]

The chert from the Castelltallat Formation (South-Central Pyrenees): Archaeometric characterization and archaeological implications

1. CSIC – Institució Milà i Fontanals, Archaeology of Social Dynamics, C/ Egipcíaques 15, 08001 Barcelona (Spain)
2. Universitat de Girona – Department de Environmental Sciences, Campus de Montilivi s/n, 17003 Girona (Spain)
3. CSIC – Institut de Ciències de la Terra Jaume Almera, Laboratory of X-Ray Diffraction, C/ Lluís Solé Sabaris s/n, 08028 Barcelona (Spain)
4. CCiTUB & CSIC – Institut de Ciències de la Terra Jaume Almera, Laboratory of Paleomagnetism, C/ Lluís Solé Sabaris s/n, 08028 Barcelona (Spain)
5. Instituto Geológico y Minero de España – Unidad de Zaragoza, C/ Manuel Lasala 44-9B, 50006 Zaragoza (Spain)
6. Universitat de Barcelona – Department of Earth and Ocean Dynamics, C/ Martí i Franqués s/n, 08028 Barcelona (Spain)
(*) Corresponding author. E-mail: terradas@imf.csic.es, Phone: +34 934426576, Fax: +34 934430071

Abstract

Chert from the limestones and marly limestones of Castelltallat Formation (Ebro Basin) was widely used throughout prehistoric times in north-eastern Iberia to produce stone tools due to its properties and accessibility. A rough estimate indicates that this rock -either as raw material or as lithic products- was distributed mainly to the north of the outcrops, over an area of 6000-8000km^2. However, other rocks in the area have similar characteristics which can lead to confusion in the interpretation of its prehistoric use and distribution. In order to establish useful archaeometric criteria for differentiating this chert from other similar, the Castelltallat chert is characterised in petrographic, mineralogical and geochemical terms.

The chert nodules are found to be homogenous at the macro- and microscopic level, with a significant presence of bioclasts, thus indicating they might be formed in a freshwater lake environment by the early diagenetic replacement of carbonates in shallow waters. The mineralogical composition is homogeneously uniform and of a flint type, characterised by an almost exclusive predominance of quartz, without any opaline phases, and a variable proportion of moganite. The iron oxide content is very low, whereas its chemical composition is unusually high in uranium which correlates positively with carbonate content and negatively with silica.

Archaeometrical parameters are provided to reach a proper identification of tools knapped with this chert. This way, chert from Castelltallat Formation turns out to be a valuable lithological marker to evaluate the range of mobility of the human groups who lived in the north-eastern Iberia and their contacts with neighbouring areas.

Keywords: Chert, Archaeometry, Ebro Basin, Castelltallat Formation, Prehistory, Human mobility

INTRODUCTION

Chert -and siliceous rocks in general- were profusely knapped throughout prehistory to make tools (Church 1994; Inizan et al. 1995; Odell 2004). Among other reasons, the widespread use of stone tools can be attributed to the hardness, conchoidal fracturing and chemical stability of chert, all of which are a consequence of its composition and crystalline structure (Bertouille 1989; Luedtke 1992; Götze 2012). Although it is far from being a scarce rock, its distribution on the Earth's surface is extremely irregular. Therefore, past human societies who needed it had to adapt, in any place and time, to its varying nature and availability in the environment.

The investigation about activities and processes connected with the procurement of chert and other raw materials provides useful information on many aspects of the organisation of prehistoric societies. Therefore, the determination of the geological and geographic origin of the rocks used as raw materials by prehistoric humans should be one of the foundations on which to propose hypotheses about the mobility of human groups and their territories and how these groups managed their resources. This type of work is expected to provide new data with which to approach the organisation of the technical procedures of past societies as well as their technological skills (Terradas 2001, 2012).

Nevertheless, in order to determine the provenance of lithic raw materials, it is necessary to establish beforehand which geological formations contain similar rocks in a given geographical area and to characterise these rocks in terms of their lithological properties, with the aim of establishing particularities that allow them to be discriminated from one another (Tarriño and Terradas 2013). As a result, attempts have been made in recent years to characterise the types of chert that outcrop in different Iberian regions and were probably most used by prehistoric communities. Some examples in the Spanish literature include studies from the Baetic System (Lozano et al. 2010; Morgado et al. 2011), Madrid Basin (Bustillo and Pérez-Jiménez 2005), Northern sub-plateau (Fuertes-Prieto et al. 2014), Cantabrian Mountains (Tarriño et al. 2013) and the Basque-Cantabrian Basin and Navarran Pyrenees (Tarriño et al. 2007, 2015).

The current situation is quite different in the Ebro Basin, where many geological formations containing siliceous rocks are attested but these are not well characterized. This region constitutes a crossroads connecting the mountain ranges of the Pyrenees with the Mediterranean coast. So it is essential to lay the scientific foundations to define each type of chert in order to be able to reconstruct the mobility of prehistoric populations throughout this region. With the goal of filling this gap we have begun to study the geological formations in the eastern sector of the Ebro Basin (Ortega et al. 2016). As part of this larger project, the present work is aimed at fully characterising the chert (flint) in the Castelltallat Formation. For this purpose, the geological and environmental setting in which it is found is described and contextualised, and a petrogenetic model for its formation is proposed. In this way, the present study contributes to the dynamics of cataloguing and characterising the main types of siliceous rocks used in the Iberian Peninsula during prehistory (see above references).

The choice of this case study is based on the fact that artefacts made of this rock are often found at prehistoric sites located in north-eastern Iberia. The material properties have been partly described by some of the researchers working in the region (e.g. Mangado et al. 2012; Roy et al. 2013). In these studies and others (Sánchez 2014; Mazzucco et al. 2013) this chert type is called *Serra Llarga Flint* after one of the relief units where it outcrops. However, the chert found at archaeological sites has been attributed to this formation without first establishing its most diagnostic petrological traits, which are distinct from similar types in other lithological units in the region. The present study aims to rectify this omission, providing a full characterization of

mineralogical, petrological and geochemical properties of the chert from the Castelltallat Formation. In addition, the uses of this chert during prehistory are discussed, based on the literature available, and a first approach to the management of the siliceous raw materials from this carbonate formation is proposed.

GEOLOGICAL SETTING

The Castelltallat Formation (Sáez 1987) is a cenozoic lithostratigraphic unit that forms part of the sedimentary fill of the Ebro Basin, a depression between the mountain ranges of the Pyrenees, the Iberian System and the Coastal-Catalan Range, in north-eastern Iberia (Fig. 1A). The origin and evolution of the basin was mainly controlled by the uplift of the Pyrenees although its sedimentary infill was also influenced by thrusting and uplift of the other ranges that surround it. The sedimentary infill reaches a maximum thickness of 4000m and dates from the Palaeogene to the upper Miocene (e.g. Gaspar-Escribano et al. 2001). The basin was filled in endorheic conditions from the Late Eocene (Costa et al. 2010), which means that it was disconnected from the sea, favouring lacustrine sedimentary systems in its central sector with a low topographic gradient, with powerful and frequent expansions and retractions, particularly suitable for the formation of chert (Bustillo 2010). Chert occurs as a common diagenetic product in both sulphate and carbonate lacustrine systems (Ortí 1990; Arenas and Pardo 1999; Arenas et al. 1999) and is often found in several lacustrine formations in the Ebro Basin. In coherence with the spatial-temporal evolution of the sedimentation in this basin, the oldest levels with chert (Palaeogene) -which is the case of the Castelltallat Formation-, correspond to the stratigraphic units that outcrop in the north-eastern part of the basin, uplifted by positive subsidence and folding and partially eroded. During the Neogene, lacustrine systems shifted to the central area of the basin.

The sedimentary fill in the Ebro basin evolved in stages as it adapted to the progress of the tectonic remodelling of the relief that forms its structural boundaries (Pardo 2004). In its eastern sector, to the east of the Cinca River, between the Late Eocene and Middle Miocene, the fill is sub-divided into five depositional sequences, each one of which belongs to the development of a lacustrine system followed by an alluvial period (Anadón et al. 1989). Lake environments depended on the orbital eccentricity. Times of lake expansion representing relatively wet periods are correlated to eccentricity maxima (Valero et al. 2014). A punctuated migration of the lacustrine systems from NE to SW occurred as a response to the balance between sediment supply and subsidence (Anadón et al. 1989; Valero et al. 2014). At the end of the lower Oligocene, after Depositional Sequence IV, sedimentation in the eastern part of the basin completely finished and it became terrigenous thereafter.

Castelltallat Formation forms part of La Noguera Lacustrine System, the first above the Eocene marine sediments in the eastern sector of the Ebro Basin (Depositional Sequence I). The system began with evaporitic sedimentation (Barbastro Fm), which changed vertically to carbonate sedimentation (Torà and Castelltallat Fms) and culminated with progradation of alluvial deposits (Solsona and Peraltilla Fms). The lacustrine deposits are progressively younger towards the west, from an upper Eocene age in the eastern sector to lower Oligocene in the west. They outcrop in the north of the Central Catalan Depression along three tectonic structures; the Tordell thrust in the east, the Súria anticline in the centre and the Barbastro-Balaguer anticline in the west (Fig. 1B).

Castelltallat Formation consists of alternating strata of limestone and marly limestone with chert nodules, and mudstones occasionally interbedded with sandstones (Fig. 2). Deposits of this formation outcrop in three separate sectors progressively younger from east to west and associated with the mentioned tectonic structures: (1) The eastern sector, to the east of Cardener River, corresponds to the carbonate sediments of the Moià

Member of Castelltallat Formation (70m thick). These carbonates are poor in chert and have not been studied in this paper. Moià Member has been dated by vertebrate fauna, charophycean flora and palaeomagnetism in the Priabonian (Upper Eocene) (Sáez 1987; Feist et al. 1994; Costa et al. 2011). (2) The central sector corresponds to the carbonate deposits rich in chert outcropping in the axis of the Súria anticline (Fig. 1B) that forms the Serra de Castelltallat. In this sector, the Castelltallat Formation reaches a maximum thickness of 250m, gradually thinning towards the west changing to carbonate siltstones of the Torà Formation (Sáez 1987). Here, the upper part of Castelltallat Formation has been assigned to Lower Rupelian (Del Santo et al. 2000). In the southern flank of the anticline, materials of the Castelltallat Formation dip to the southeast at angles varying from 10º to 80º. (3) The western sector, separated 35km from the central sector (Fig. 1B), has carbonate materials rich in chert with a stratigraphic continuity of nearly 95km. Its maximum thickness of 75m in the Serra Llarga decreases progressively towards the west. At the end of the western sector this unit possesses, at least in part, a lateral equivalent with carbonate siltstones of Torà Formation, all below the Peraltilla Formation alluvial sediments (Macias et al. 1987; Luzón and Rodríguez 2003). In this sector these beds dip towards the south, at variable angles that become quite steep (65º to 75º).

Sediments of Castelltallat Formation were deposited in a shallow lake rich in carbonates with little bathymetric gradient, which developed in the distal part of large fluvial fans systems attached to the Pyrenean and Catalan Coastal Range basin margins (Sáez et al. 2007). The limestones and marly limestones bearing chert nodules belong to two facies (Sáez 1987; Cabrera and Sáez 1987): (1) light grey mudstone textures with ostracods and charophyte remains, sometimes with root marks, laid in beds about 10cm thick, that are grouped in packets a metre to tens of metres thick and extend over a kilometre (facies Lm), and (2) dark grey wackestones and packestones textures rich in organic matter (facies Lw), sometimes sandy and erosive on the Lm facies beds, with frequent carbonised root marks and remains of gastropod shells. They form thin, lenticular beds that extend over a metre to tens of metres and which are thinner and less frequent than those of the Lm facies. Fine -terrigenous dominated- beds are grey, blue or yellowish mudstones that contain more or less carbonate (facies Md), with a massive or laminate texture, sometimes with ripple-type lamination. They are mainly composed of quartz and phyllosilicates (smectite, illite and chlorite) and to a lesser extent feldspars. All of the materials in the formation are typically ordered in shallowing lacustrine sequences about a metre thick. The most complete sequences consist of; (1) a lower interval of Lm facies, characteristic of offshore lacustrine environments, (2) an intermediated of littoral lacustrine facies (Lw), and (3) an upper interval of grey-blue mudstones (Md) deposited in a plain, periodically flooded, which surrounded the lake and was fed by the distal parts of the fluvial fans (Sáez et al. 2007).

PREHISTORIC USES OF CASTELLTALLAT CHERT

Castelltallat chert is one of the rocks in north-eastern Iberia whose properties are best adapted to the manufacture of stone tools by means of knapping. Its availability in the hills of Serra Llarga, with easily visible and accessible outcrops, as well as its location on the crossroads between the Ebro valley and some of its tributaries, like the Segre and the Noguera Ribagorzana rivers, mean that it was likely to be a potential resource for the prehistoric populations in the area.

The archaeological record confirms that it was indeed used repeatedly in the region throughout prehistory (Fig. 3). However, as we stated before, chert found at archaeological sites has been often attributed to this formation without using preview characterization studies, by means of *visu* identification or macroscopical approach.

Evidence of its use in flake production has been found in Middle Palaeolithic occupations such as Cova del Estret de Tragó (Parcerisas 1999) and the rock-shelter of Roca dels Bous (Martínez et al. 2010), where it complements the use of other mineral resources located in the immediate surroundings of the sites. Its use then appears to increase quantitatively in the Upper Palaeolithic and Mesolithic related to the production of blade blanks, although it continues to complement other local resources. Thus it has been documented in the eastern Pre-Pyrenees at Cova Gran de Santa Linya (Roy et al. 2013), Cova del Parco (Mangado et al. 2014) and Balma Guilanyà (Martínez and Mora 2009) and to a lesser extent in the central Pre-Pyrenees at Cova Alonsé and Abrigo de Forcas I (Sánchez 2014). Evidence has also been found at some Pyrenean sites, at the head of the Segre River, such as the open-air settlement of Montlleó in Cerdanya (Mangado et al. 2014) and Balma Margineda in Andorra (Lacombe 2007). Finally, this chert continued to be used, mainly for blade production, in the Neolithic, as recorded at Cova Colomera (Mangado et al. 2012) and Cova del Sardo (Mazzucco et al. 2013).

The open-air Neolithic settlement of Auvelles (Castelló de Farfanya), at the foot of the eastern outcrop of the Castelltallat lithological unit, where the chert in this formation was used predominantly, deserves a special mention. Mangado et al. (in press) suggest that the domestic structures recorded at the site might be linked to the thermal treatment of the chert, a procedure applied in other geological and geographic contexts to enhance chert's suitability for knapping. However, a specific experimental protocol (Boix 2012) was able to show that this chert was not altered by heat in this site. Additionally, in the proximity of the settlement, in the Montvell Hills, chert quarries exploited in the Castelltallat carbonate beds have recently been discovered and excavated. Although the age of these quarries cannot be established precisely, the evidence suggests that they might date to Neolithic times (Terradas et al. in press).

In the region of the Pyrenees where its geographic distribution in prehistory is attested within a surface area of about 6000-8000km^2, Castelltallat chert forms a lithological type easily identified in archaeological assemblages. This is because continental sedimentation in the intra-mountain basins in the Pyrenees did not develop widely in lacustrine sedimentary environments. Only the Tremp Formation (Rosell et al. 2001; López-Martínez et al. 2006) includes limestone formed in transitional lake environments which, locally, contains chert that is comparable in some aspects (the micro-paleontological record and the petrographic facies) to Castelltallat chert. Nevertheless, based on the macroscopic appearance of the two chert types it is easy to discriminate them (see, for example, Roy et al. 2013), even though they were both often used at the same archaeological sites.

In contrast, it is very difficult to identify the artefacts made in chert from the Castelltallat unit at sites in the eastern part of the central Ebro Basin plain. That is the case, for instance, of the Bronze Age settlement of Minferri in Juneda (Palomo et al. 2012), where the local communities were able to procure similar chert from other carbonate units in the Ebro Basin. These are the Montmaneu (Ortega et al. 2016) and Torrent de Cinca (Luzón and González 2000) Formations, where chert with very similar genetic and compositional characteristics occurs. The reach and regularity of its distribution to the south of the outcrops is therefore still unknown, and it is necessary to carry out specific studies on the chert types in archaeological assemblages in this geographic area. This would contribute towards a better characterisation of the various uses of this mineral resource and its diachronic variation, and would determine its distribution area more precisely.

METHODS

The chert from the Castelltallat Formation has been analysed using the petrographic, mineralogical and geochemical techniques normally applied in the characterisation of siliceous rocks (e.g. Luedtke 1992; Bustillo et al. 2009; Tarriño and Terradas 2013). The chert samples have also been characterized using rock magnetic methods which have proved useful for assessing chert quality and provenance in previous studies from the Basque-Cantabrian basin (Larrasoaña et al. 2016) and other regions in Portugal, in North America and the United Kingdom (Borradaile et al. 1998; Thacker and Ellwood 2002).

In order to assess variability in this chert type, 11 samples from two different locations have been analysed: 6 from Cal Mestre (CM) in the Serra de Castelltallat (near Calaf village), in the central sector of the formation, and 5 from Tossal del Castell (TC) in Serra Llarga (Castelló de Farfanya), in the western sector (Fig. 1B). Samples come from the highest section of the unit, where beds containing more density of chert nodules occur. The precise stratigraphic location of the samples can be seen in the stratigraphic logs drawn in figure 2. Given the distance reached by this unit and its lateral stratigraphic equivalents, the complete characterization (i.e. intraformational variability) of this chert should be considered as preliminary. However, taking into account the analytical approaches applied, we consider this study constitutes a solid basis for the petrological characterization of Castelltallat chert while further analyses will doubtlessly contribute to a more precise determination of its intra-formation variability.

In accordance with the protocols established in the Catalan Siliceous Rock Lithotheque (LITOcat) (Terradas et al. 2012), the samples were taken and referenced within the stratigraphic schemes and sections in the literature. In this way, the samples benefitted from the geological information and interpretation of each site. The reference number for each sample corresponds to its inventory number in the LITOcat collection, except where indicated.

The petrographic characterisation of the samples was performed in the archaeology laboratories at Institució Milà i Fontanals (IMF-CSIC, Barcelona) after the thin sections were prepared in the Thin Section Preparation Laboratory in the Autonomous University of Barcelona. In turn, the mineralogical analysis of the samples was carried out at the X-Ray Diffraction Service of the Institute of Earth Sciences Jaume Almera (ICTJA-CSIC, Barcelona). For this purpose, all the samples were pulverized and carefully homogenized. X-ray powder diffraction (XRPD) measurements were performed with a Bruker D-5005 diffractometer (Bragg-Brentano $\theta/2\theta$ geometry), equipped with a 2.2kW sealed Cu X-ray source (Cu Kα radiation), a Ge secondary monochromator, Soller slits and a NaI (Tl) scintillation detector. XPRD scans were acquired from 4º to 60º in 2θ, with 0.05º steps and an integration time of 3s per step. For the identification of the crystalline phases, the International Centre for Diffraction Data (ICDD) PDF-2 database was used. Quantitative phase analyses (QPA) were carried out with the Rietveld method (Young 1993), which also allowed us to evaluate the coherence length of the quartz micro-crystalline domains. The Rietveld analyses were carried out by using the fundamental parameters approach in order to calculate the theoretical diffraction spectra. A Lorentzian convolution was introduced to evaluate the size of the microcrystalline domains (L). For the Rietveld refinements, the TOPAS 4.2 programme (Bruker AXS) was employed.

Rock magnetic analyses were conducted in the Barcelona Paleomagnetic Laboratory (CCiTUB-ICJTA CSIC). Raw chert samples were cut into $8cm^3$ cubes in order to adapt them to the sample holders of the equipment used. Reliable magnetic measurements can be measured also for archaeological artefacts, provided their shape do not

depart too much from the ideal shape that avoids anisotropy effects on magnetic measurements (e.g. height = 0.82 x diameter, see Borradaile et al. 1998). In this case, archeological artefacts with the most regular shape need to be selected optimizing also their size, in order to get magnetic measurements well above the resolution thresholds of instruments. The parameters measured were, in this order, the low field magnetic susceptibility (χ), and two isothermal remanent magnetizations induced at fields of 0.3T (IRM@0.3T) and 1.2T (IRM@1.2T). IRM@1.2T has been used as a proxy for the concentration of magnetic minerals *sensu lato*, for which a first indication is provided by χ (Liu et al. 2012). The forward S ratio, defined as IRM@0.3T/IRM@1.2T (Kruiver and Passier 2001), has been used to constrain the relative ratio between high- and low-coercivity minerals. All measurements were normalized by the weight of the samples. χ was measured with a Kappabridge KLY-2 (Geofyzica Brno) using a field of 0.1mT at a frequency of 470Hz. IRM@0.3T and IRM@1.2T were produced using an IM10-30 (ASC Scientific) pulse magnetizer and then measured using a SRM755R (2G Enterprises) three-axes cryogenic superconducting rock magnetometer. Following Larrasoaña et al. (2016), and in order to account for the possibly skewed distribution of rock magnetic parameters, their median values and the associated interquartile ranges have been calculated to display average values and associated errors.

The geochemical analyses were performed at the ALS commercial laboratories. The detailed description of the protocols and equipment used can be consulted on their website (http://www.alsglobal.com/). Major oxides, trace elements and rare earths were determined using ICP-AES and ICP-MS (laboratory method ref: ME-ICP06, ME-MS81 and ME-MS42) which use lithium-borate fusions and digestions by four acids and aqua regia in the preparation of the samples. The total content in carbon (C-OR07) and sulphur (S-IR08) and weight loss on ignition (LOI) were calculated with sequential heating techniques in a furnace. The concentration of the latter has been normalised using the mean North American shale composition (NASC index) (Gromet et al. 1984). The indices reporting significant anomalies of cerium (Ce/Ce*) and europium (Eu/Eu*) (Taylor and McClennan 1985), La_n/Yb_n which reflects the relative enrichment of light vs heavy REE, and La_n/Ce_n which informs about the chert depositional environment (Murray 1994) have also been calculated.

Finally, scanning electronic microscopy (SEM) was used to observe the superficial alteration causing white patina on the chert, which is a very common phenomenon in the Castelltallat Formation. A Zeiss DMS 960A microscope was fitted with an X-ray microanalysis system of energy separation (EDX) Link Isis L 200 B with a silicon sensor (Li) capable of detecting elements with an atomic number of 6 or more. These analyses were performed in the Microscopy Service at the University of Girona.

The results of the geochemical analyses were studied with variance analysis statistical techniques (one factor ANOVA) and bivariate correlations. These are able to (1) indicate chemical composition differences between sample locations and (2) identify significant compound associations. Chert samples from the formation, the preparations and residue of their processing, as well as laboratory reports and other documentation, are archived in the LITOcat collection, where they may be consulted, waiting for the website to be enabled.

RESULTS

The studied chert is hosted within the limestone and marly limestone beds (Ld, Lw facies), and are macroscopically similar across the entire Castelltallat Formation. Silicification produced nodules with an average diameter of 8 to 10cm, with a flat, elliptical or slightly botryoidal shape, which are found in layers parallel to the stratification in the rocks and often at the top of the beds (Fig. 4). Locally (in CM) silicification caused stratiform

concretions due to the coalescence of adjacent nodules. The proportion of chert nodules is variable from bed to bed, and is largest (with nodules up to 20cm in diameter) in the highest section in the unit (Fig. 2). Although they contain joint surfaces or sets owing to the tectonic forces suffered by the limestone in the unit during its folding, this barely affects their conchoidal fracturing.

The chert is dark brown to black in colour, opaque, finely-grained and normally with a massive texture (Fig. 5A). Some nodules are banded concentrically, a trait that is often hidden and usually increases through a slight alteration to the fresh section of the rock (Fig. 5B). The nodules are covered by a thin layer of carbonate (<1mm) which is strongly adhered, smooth and clearly separate from the homogeneously silicified interior. When it is altered, the chert develops a white patina that is due to the development of secondary porosity through the porosity in the rock's texture (Fig. 6).

Observation with a petrographic microscope reveals that Castelltallat chert is formed by a mosaic of granular quartz of micro-and crypto-crystalline size (<20μm) which encloses a variable amount of relict carbonate inclusions (0.5-5%). The fill of the primary porosity contains mosaics of isometric megacrystalline quartz and fine bands of length-fast chalcedony, in the typical sequential arrangement according to the order of their successive crystallisation in phases (with the megaquartz mosaics last) (Fig. 5E). The fissures, where they exist, are filled by megacrystalline quartz or calcite (sparite).

The nodules are of mudstone to wackestone texture and normally contain less than 5% allochems. These include bioclasts and to a lesser extent opaque minerals as well as micrite. The bioclasts are present in large numbers, and can be observed *de visu* in hand samples. Viewed under a binocular microscope and petrographic microscope, the same elements as in limestone and marly limestones can be identified: ostracod shells, stems and gyrogonites of charophyte algae, and occasionally gastropod shells (planorbids). All together, they are indicative of a freshwater lacustrine environment. The gastropod shells, when they are not infilled, cause the macroscopic-size moldic porosity.

The bioclasts do not display selection according to grain size or any particular orientation. The ostracod and gastropod shells are either whole or fractured, but never flattened (Fig. 5E). The primary aragonite microstructure of the gastropod shells is pseudomorphised by lutecite, which indicates an early silicification of the sedimentary deposit (Bustillo 2010; Jacka 1974). This must have occurred before its deep burial, as they show no signs of significant mechanical compaction. The charophyte stems, which have poor resistance to transportation, are well conserved, suggesting their formation in shallow environments (Wright 1990) (Fig. 5D).

The mineralogical study by XRPD reveals the similarity between the samples investigated in this work. The diffraction spectra allowed us to identify in all the samples the majority presence of cryptocrystalline quartz, together with small amounts of calcite. In the TC samples, the diffraction scans also display a small peak that can be attributed to moganite. In contrast, in the CM samples moganite can only be identified in one sample (109CM). Our Rietveld analyses indicate that the quartz content of all the studied cherts is over 88% in weight, and approaches 99% in the particular case of CM samples. The calcite content is less than 6% in the TC samples and, on average, it is even smaller in the CM samples (~1-2%).

It must be borne in mind that moganite is a metastable phase of silica that appears in chert of different origins, ages and sedimentary environments, both marine and continental (Heaney and Post 1992; Graetsch and Grünberg 2012). Although moganite is often associated with arid environments, it is not of special significance when it amounts to less than 20% of the total rock volume (Bustillo 2002). Despite the typical error of Rietveld

refinements dealing with moganite is quite high owing to the fact that the diffraction peaks of this phase overlap with those from quartz, semi-quantitative data can be estimated from such analyses. We find that the samples from TC contain about 4-6% moganite, whereas sample 109 from the CM sector contains about 2% of this phase. These values are similar to those reported in chert from the same formation in Algerri (western sector) (Roy et al. 2013), where moganite contents between 2 and 7% were reported.

The Rietveld analyses also provide information about the structural properties of the chert minerals and, in particular, about quartz. Table 1 shows the size (*L*) of the microcrystalline domains of quartz for all the samples studied in this work, as obtained after the Rietveld refinements. The values obtained, ranging from 65 to 90nm, are typical of cryptocrystalline material, and are not too different from the values found on material from chert outcrops with similar characteristics (Ortega et al. 2016). The samples analysed in the present work do not contain opal (opal A or opal C-T), probably because the opal phases completely recrystallized as quartz during the chert maturing process. It is likely that moganite also underwent a similar recrystallization process. In fact, it is noteworthy that the size of microcrystalline domains (*L*) tends to be larger in the samples with less moganite (Table 1), which might be related to the progressive recrystallization and conversion of moganite to microcrystalline quartz, ending up with subdomains with greater coherence lengths, i.e., higher crystallinities.

The results of the magnetic measurements are summarized in Table 2. χ values range from -3.49 x 10^{-10} to -2.27 x $10^{-9}m^3/kg$, with median values of -0.35 x $10^{-9}m^3/kg$ and -4.08 x $10^{-9}m^3/kg$ for the TC and CM subsets respectively (Fig. 7A). These negative values are lower but similar to the reported value for pure quartz (-0.62 x $10^{-8}m^3/kg$, Dunlop and Özdemir 1997) and for diamagnetic-dominated chert samples from Northern Spain (Larrasoaña et al. 2016; Ortega et al. 2016), the United Kingdom, United States of America and Portugal (Borradaile et al. 1998; Thacker and Ellwood 2002), and are much lower than those measured for more magnetic chert elsewhere (Fig. 7A). This indicates that quartz dominates the magnetic properties of the studied chert due to its purity, which can therefore be considered as flint (sense Borradaile et al. 1998). It is worth pointing out that S ratios for samples from TC and CM are very different. Typical S ratios >0.9 for the TC subset indicate that low coercivity minerals (e.g. magnetite) are the dominant ferromagnetic minerals in this chert. Conversely, S ratios for the CM samples are much lower and are characterized by a much larger variability (Fig. 7B). This suggests a much more heterogeneous magnetic mineral assemblage that is characterized by the dominance of high coercivity minerals (e.g., hematite and/or goethite) over magnetite (Larrasoaña et al. 2016). Only samples 186 and 187 from the CM sector show S ratios >0.9, similar to the TC ones. Noticeably, these samples are characterized by IRM@1.2T intensities that are much larger than those from TC, so that both populations are clearly distinguishable from each other in a plot relating S ratios and IRM@1.2T intensities (Fig. 7B). The overall lower IRM@1.2T intensities of the TC samples are readily visible also in Fig. 7C, where χ is plotted as a function of the log of the IRM@1.2T (see Borradaile et al. 1998). Both the TC and CM subsets fall in the range of other diamagnetic-dominated chert types in Northern Spain (Larrasoaña et al. 2016; Ortega et al. 2016), the United Kingdom, United States of America and Portugal (Borradaile et al. 1998; Thacker and Ellwood 2002), which provides further evidence of their purity (Larrasoaña et al. 2016).

The geochemical analysis shows that the chert consists mainly of SiO_2 (mean of 91.59%). The most common impurities are CaO and, to a lesser extent, Fe_2O_3 and Al_2O_3 (Table 3). The fraction of the rock volume lost in the ignition of the samples (LOI value) is greater than the CaO content for all of them. The LOI correlated almost 1

to 1 with the total carbon content (Total C), from which it can be deduced that the samples must contain a significant amount of organic matter (~1.5%).

The trace elements found in appreciable amounts (mean >5ppm) are Sr, Ba, U, Cu, Zr and Zn, in order of concentration, from more to less. They all appear in a smaller proportion than the amount of each element in the Earth's crust as a whole (Mason and Moore 1982), except U, which is above that reference value, and As, Sb and Ag (the latter only in the CM samples). The TC samples, which are more siliceous, contain more Ba and Zn than the CM samples, which in turn contain more carbonates, Sr, U and Ag.

The U content in the samples varies from 2.84 to 65.50ppm (minimum and maximum, respectively) in a range that exceeds the order of magnitude, which in itself is not infrequent (see for example Bustillo et al. 2012). The CM samples contain a mean of 54.82ppm U whereas the TC samples only 4.10ppm. ANOVA statistical tests verify the significant difference according to the place of sampling (t_5=13.66, $p>0.05$). Considering all the data together, U correlates positively, with a statistically significant level, with the CaO content and the LOI ($r>0.7$), and to a lesser extent, with Sr, MgO, Na_2O and K_2O ($r>0.5$). In contrast, it correlates negatively and significantly with Ba, Zn and Bi ($r>-0.8$) and weakly with SiO_2 y Fe_2O_3 ($r>-0.5$) (Table 4).

It must be noted that the rare earths (REEs) are all represented well below the value corresponding to each type in the NASC reference pattern (Table 5). With a mean value for ΣREE of 3.67ppm, the chert is therefore impoverished in REEs. No significant differences are observed according to the source area (t_5=1.42, $p>0.05$). All the elements in the group correlate positively with each other, and except for the three heaviest (Tm, Yb, Lu), also with ΣREE ($r>0.9$; $p>0.01$). One by one, however, none of them correlates statistically significantly with any other major or trace element. Only Al_2O_3 ($r=0.948$; $p>0.01$) and, less intensely, Fe_2O_3 ($r=0.518$) correlate positively with ΣREE, which points to their known absorption in clay minerals and iron. Al_2O_3 as well as La and Ce, the elements in the group found in largest amounts, closely fit the model of linear regression that explains their covariance with ΣREE.

The NASC-normalised REEs concentration diagram displays a distinctive flat form (Fig. 8). This is similar to that of the reference pattern and also the one that corresponds to the sediment load in suspension in rivers (Piper and Bau 2013). The graph does not show any apparent anomalies in Ce and Eu (the latter was only measured for two samples). The Ce/Ce* index varies between 0.74 and 0.88, and the Eu/Eu* index between 0.83 and 0.89, both of them close to 1. The La_n/Ce_n index varies in the 1.26-1.86 range, with a mean of 1.5, which agrees with the REEs being brought by continental water flow not especially low in Ce and detritic input from the same origin that is shown by the correlation between ΣREE and clays and iron. Finally, the La_n/Y_n index, with a mean of 1.6, indicates that there is no relative fractioning of the REEs, which is also consistent with the above.

DISCUSSION

Uranium content

While it is not the most common impurity in siliceous rocks, it is not unusual to find traces of U in them (e.g. Matteson et al. 2005; Moh'd and Powell 2010; Bustillo et al. 2012). However, the chert in the Castelltallat Formation contains a significantly high mean U content (18.1ppm), which multiplies by a factor of 10, and in several samples by even more, the mean amount of U in the Earth's crust (1.8ppm, approximately equivalent to 3mg kg^{-1}) (Massey et al. 2014).

In the samples, U correlates positively with the CaO content and negatively with SiO_2. These correlations are the opposite of those that Bustillo et al. (2013) found in the geochemical composition of silicifications in silcrete in the Madrid Basin. According to these authors, U would not have been originally located in the carbonates but would be associated with the siliceous phases that replaced them. To be precise, the absorption of U would initially be produced by organic matter (live rooted vegetation). The decomposition of this organic matter would have induced the silicification (by a drop in pH) and would have mediated the transference of U to the opaline phases, the precursor of the chert, which would have been effective absorbers of U (Massey et al. 2014).

The dissimilar association of CaO and SiO_2 with U in the chert samples from the Castelltallat Formation therefore suggests a different route for its addition to the chert and a petrogenetic model of silicifications that was also different.

The crystallochemical properties of the U ions inhibit the replacement association of U in the quartz α structures (Götze et al. 2015). In contrast, U ions easily replace Ca in calcite and aragonite and form complex uranyl compounds when they associate with organic matter (Barnes and Cochran 1991; Sturchio et al. 1998; Meece and Benninger 1993).

The most probable source areas for the U content in the Castelltallat chert are the granite and hypabyssal rocks outcropping in the axial zone of the Pyrenees and in some parts of the Catalan Coastal Range, as in certain sections of the Permian and Triassic detritic sedimentary units in both mountain ranges, which are rich in this element (Arribas 1992; Castillo et al. 2009).

The alluvial systems in the hydrographic basins of these geological units were able to bring U to the lakes and groundwater together with the other detritic and dissolved matter in their sedimentation. The presence of U in high proportions is not widespread in the whole sedimentary fill of the Ebro Basin, but only appears in certain places and at specific periods, one of which is the Castelltallat Formation.

Once it had been introduced in the basin, part of the U may have been reduced into an authigenic mineral type – typically U (IV) – susceptible of being sequestered in the sediment and from there moving into the silicifications. Yang et al. (2015) noted that the main factors controlling the retention of U in the sediment of carbonate lacustrine systems are the oxygen content and the organic matter input. They show that in the carbonate facies in Lake Qaidam (Tibetan Plateau in western China) U correlates with carbonates and Sr, just as in the present case. These authors conclude that, based on the joint temporal variation of these elements, U was controlled by the mineralogy of the carbonates in the system. They also note that the retention of U does not require deep and especially reducing sedimentary environments. Chappaz et al. (2010) indicate that most of the recycled U in the sediment of continental lacustrine systems corresponds to lithogenic U particles. They also find that the authigenic U fraction, in the absence of competitive absorbent mineral (hydroxide Fe in the examples they cite) tends to associate with organic matter, in both oxidising and reducing environments.

Therefore the silicifications in the central and western sectors of the Castelltallat Formation would take U from the carbonate sediment, and its proportion is higher where this originally contained a larger proportion of organic matter. Although the presence of high concentrations of U in chert is normally interpreted as indicative of reducing conditions during its formation (Luedtke 1992), the fact is that the sequestering of U in carbonate sediment does not require such conditions.

A genetic model for the formation of chert in the Ebro Basin

Formation of chert nodules in Castelltallat Formation is closely linked to offshore and littoral shallow lacustrine conditions (Lm and Lw facies respectively) but also as a consequence of the cyclical drop in lake water level, affecting facies that were originally less shallow (Lm facies). According to the model proposed by Knauth (1979, 1994) for the petrogenesis of nodular chert, its formation can be explained by the particular conditions in carbonate lacustrine sediments when they are at shallow depth. In these permeable materials, meteoric water saturated in silica (surface run-off and groundwater feeding the system) mixes with the water in the sediment (sub-saturated in silica and saturated in calcite). Its dilution produces a mixture sub-saturated in calcite and saturated in silica. In this way, the local hydrogeological conditions are created, in a relatively confined environment, for the start of silicification. In littoral lacustrine environments with greater biological productivity, in which these hydrological conditions arise, the continual arrival of organic matter also contributes to a decrease in the pH of the diagenetic aqueous solutions (Siever 1962), favouring the precipitation of silica and increasing the solubility of calcite (Hesse 1989).

The silica in the chert probably has a biogenic origin. It is generally thought that the main source of soluble silica in continental environments are plant phytoliths and to a lesser extent, the frustules of diatoms (Conley 2002; Loucaides et al. 2008). Meteoric water feeding the lake could gradually be enriched in silica until it reached saturation, as it carried phytoliths from the soil at the head of the drainage basin to the lake.

The REE profile of the chert samples confirms the nature of this flow, which is indeed implicit in the general sedimentological model of the carbonate lacustrine systems in the Ebro Basin. The hydric flow would only attain the appropriate conditions for the precipitation of silica in shallow littoral lakes, due to the greater acidity of the water caused by the acids derived from the decomposition of organic matter. The oblate form of the concretions indicates that their formation was produced by the advection of phreatic currents (McBride et al. 1999), which supports the genetic model proposed here.

Intra-formation variability

The comparative analysis of the samples from the eastern sector of the formation (Cal Mestre site: CM) and the western sector (Tossal del Castell: TC) suggests that despite their macro- and microscopic homogeneity, the cherts display certain intra-formation variability in their composition: 1) All the TC samples contain moganite (4-6%), whereas it was found in only one CM sample and in a smaller proportion (2%); 2) The TC samples are a little more siliceous and richer in Ba and Zn than the CM samples, which contain more carbonates, Sr and Ag; 3) The most notable composition difference lies in the U content as the TC samples contain a much smaller mean content (4.10ppm) than the CM samples (54.82ppm); and 4) Rock magnetic analyses have revealed significant differences between the two groups of samples as they indicate a predominance of low coercivity minerals (e.g. magnetite) in the ferromagnetic minerals in the TC samples, whereas high coercivity minerals (e.g. hematite and/or goethite) predominate in the CM samples.

This intra-formation variability may be explained by slight variations in the hydrochemical properties of the water flowing into different parts of the lacustrine system, probably connected with lithological heterogeneity in the drainage basins of surface water and/or in recharge zones and flow in underground water. In the specific case of U, the highest values may also indicate environments with greater biological productivity.

In any case, to be able to discern whether an archaeological sample comes from one or other sector of the stratigraphic unit, it will be necessary to carry out further sampling in the formation in order to corroborate the differences noted here.

Archaeological implications

To identify raw materials at a regional level, it should be pointed out that the U content in the chert from the Castelltallat Formation is probably not sufficiently useful to differentiate it from chert formed in other units of the sedimentary fill in the Ebro Basin. The reason is that U is an element brought to the basin from its surrounding area, and this process was similar throughout the whole basin. For instance, the lacustrine levels of the Calaf Formation, geographically and temporally close to the Castelltallat Formation, are equally rich in U (Martin 1974) although they do not contain chert.

In the same way, the micropaleontological content and texture of the mineral, although they allow the Castelltallat chert to be discriminated from the chert coming from the Pyrenean intra-montane basins to the north of the Ebro Basin, are probably not sufficient to differentiate it from the chert in other units of the same basin. Therefore, the recognition of these chert types in assemblages from archaeological sites in the central and eastern pre-Pyrenean and Pyrenean valleys is more successful. Although it was used as a raw material for production of tools from the Middle Palaeolithic onwards, it was in later stages of the Upper Palaeolithic when this chert was distributed most widely (Fig. 3), as it was used to make tools from blade blanks. However, the methods used to obtain this raw material from its geological substrate changed significantly in the Neolithic, as at that time quarries were opened to extract the chert. This suggests a more intensive and specialised use at that time.

CONCLUSION

The chert from the Castelltallat Formation is a diagenetic siliceous rock produced by the early replacement of carbonates in shallow littoral lacustrine environments. The textural, compositional and micropaleontological traits of the rock define it as a particular petrological type that inherited characteristics of the sedimentary facies in which it formed, and these were in turn influenced by the palaeogeography and palaeohydrology of the lacustrine basin.

In short, it is a highly siliceous and mature rock as it does not include opaline phases. It contains a low and variable proportion of moganite, although this does not appear to imply any particular environmental or genetic pattern. The main impurities are micrite, organic matter and, in a smaller proportion, phyllosilicates, all of them in low proportion as is common in flint type cherts. The content in iron oxides is also very low. Nevertheless, differences in the concentration and type of iron oxides have been observed between samples from Tossal del Castell and Cal Mestre localities as indicated by their S ratios and IRM@1.2T intensities. Chert coming from Tossal del Castell is dominated by low coercivity minerals, such as magnetite, whereas chert from the Cal Mestre sector is characterized by high coercivity minerals, such as hematite or goethite. Therefore, a combination of S ratios and IRM@1.2T values appears to be a useful tool to discriminate the provenance of these two chert sources. The chemical composition reveals a long list of elements, among which the most significant is U, which probably came from the mountain ranges around the Ebro Basin. The profile of the rare earths in the chert, which is distinctively flat, indicates they were brought by surface meteoric flow. This flow must have also brought the U and the biogenic silica that precedes silicification and which, in our opinion,

contributed to the origin of the silicifications. The correlations of U with other elements suggest that it must have been sequestered in the carbonates, partly linked to organic matter.

The physical and mechanical properties of the Castelltallat chert make it suitable for knapping and the production of lithic tools. Because of this, and due to the easy access to the outcrops, it was widely used as a raw material by prehistoric populations in north-eastern Iberia. Although it was used since the Middle Palaeolithic, the distribution area of this chert appears to increase during the Upper Palaeolithic and Mesolithic, and it is used even more intensely in the Neolithic, the period to which the Montvell quarries can be attributed. The frequency and size of the distribution area towards the south, in the Catalan Central Depression is uncertain; however, its distribution towards the north is well known and may even have crossed the Pyrenees. Despite the fact that other formations containing chert exist in this area, tectonic folding in the Pyrenean area and the low plasticity of its host rock caused numerous fractures and joint sets in the chert, which hindered the production of blade blanks of significant size from the nodules. For this reason, in this area Castelltallat chert turns out to be a valuable lithological marker indicating the range of the mobility and contacts of the human groups who dwelled in the region.

The petrographic, mineralogical, geochemical and magnetic parameters that characterise the chert in the Castelltallat Formation have been determined precisely. Some of them may be regarded as diagnostic in order to differentiate it from other chert types with similar genetic and compositional characteristics. These criteria will be very helpful in the determination of the mobility of prehistoric populations within the crossroads constituted by the Ebro Basin. An exhaustive re-examination of archaeological assemblages in accordance with the results of the present study should be able to determine with greater precision the nature and intensity of the prehistoric use of Castelltallat chert, an aspect on which we continue to work and that lies beyond the scope of the present paper.

FUNDING SOURCES AND ACKOWLEDGEMENTS

The fieldwork to obtain rock samples and the analysis of the samples was co-funded by the Direcció General del Patrimoni Cultural de la Generalitat de Catalunya and IMF-CSIC, within the framework of an inter-institutional collaboration agreement for the development of the Catalan Lithotheque of siliceous rocks (LITOcat project). Specific studies on the petrological characterisation of Castelltallat chert and its prehistoric use were carried out within the research project *'Aprofitament prehistòric i històric del sílex a Catalunya: contextos extractius i de primera transformació'*, funded by the Department of Culture of the Government of Catalonia (ref. núm. 2014/100778). The significance of human use and scope of distribution of Castelltallat chert are being approached within the project *'Productions, technical variability and technological innovation in the Neolithic'*, funded by the Spanish Ministry of Economy and Competitiveness (Grant HAR2016-76534-C2-2-R).

The authors would like to thank the anonymous reviewers of the paper for the corrections and suggestions that have contributed to improving it.

REFERENCES

Anadón P, Cabrera L, Colldeforns B, Sáez A (1989) Los sistemas lacustres del Eoceno superior y Oligoceno del sector oriental de la Cuenca del Ebro. Acta Geologica Hispanica 24: 205–230

Arenas C, Pardo G (1999) Latest Oligocene-Late Miocene lacustrine systems of the north-central part of the Ebro Basin (Spain): Sedimentary facies model and palaeogeographic synthesis. Palaeogeography, Palaeoclimatology, Palaeoecology 151: 127–148. doi: 10.1016/S0031-0182(99)00025-5

Arenas C, Alonso Zarza AM, Pardo G (1999) Dedolomitization and other early diagenetic processes in Miocene lacustrine deposits, Ebro Basin (Spain). Sedimentary Geology 125: 23–45. doi: 10.1016/S0037-0738(98)00146-8

Arribas A (1992) Yacimientos españoles de Uranio. In García Guinea J, Martínez Frías J (eds) Recursos minerales de España. CSIC, Madrid, pp 1403–1419

Barnes CE, Cochran JK (1991) Geochemistry of uranium in Black Sea sediments. Deep Sea Research Part A. Oceanographic Research Papers 38: 1237–1254. doi: 10.1016/S0198-0149(10)80032-9

Bertouille H (1989) Théories physiques et mathématiques de la taille des outils préhistoriques. CNRS, Bordeaux

Boix J (2012) El tratamiento térmico en rocas silíceas, un procedimiento técnico para la talla. Trabajos de Prehistoria 69: 37–50. doi: 10.3989/tp.2012.12078

Borradaile G, Stewart JD, Ross WA (1998) Characterizing Stone Tools by Rock-Magnetic Methods. Geoarchaeology 13: 73–91

Bustillo MA (2002) Aparición y significado de la moganita en las rocas de la sílice: una revisión. Journal of Iberian Geology 28: 157–166

Bustillo MA (2010) Silicification of continental carbonates. In Alonso-Zarza AM, Tanner LH (eds) Carbonates in continental settings: geochemistry, diagenesis and applications. Elsevier, Oxford, pp 153–178

Bustillo MA, Pérez-Jiménez JL (2005) Características diferenciales y génesis de los niveles silíceos explotados en el yacimiento arqueológico de Casa Montero (Vicálvaro, Madrid). Geogaceta 38: 243–246

Bustillo MA, Castañeda N, Capote M, Consuegra S, Criado C, Díaz-del-Río P, Orozco T, Pérez-Jiménez JL, Terradas X (2009) Is the macroscopic classification of flint useful? A petroarchaeological analysis and characterization of flint raw materials from the Iberian Neolithic mine of Casa Montero. Archaeometry 51: 175–196. doi: 10.1111/j.1475-4754.2008.00403.x

Bustillo MA, Pérez-Jiménez JL, Bustillo M (2012) Caracterización geoquímica de rocas sedimentarias formadas por silicificación como fuentes de suministro de utensilios líticos (Mioceno, cuenca de Madrid). Revista Mexicana de Ciencias Geológicas 29: 233–247

Bustillo MA, Plet C, Alonso-Zarza AM (2013) Root calcretes and uranium-bearing silcretes at sedimentary discontinuities in the Miocene of the Madrid Basin (Toledo, Spain). Journal of Sedimentary Research 83: 1130–1146. doi: 10.2110/jsr.2013.85

Cabrera L, Sáez A (1987) Coal deposition in carbonate rich shallow lacustrine systems: The Calaf and Mequinenza sequences (Oligocene, eastern Ebro Basin, NE Spain). Journal of the Geological Society 144: 451–461. doi: 10.1144/gsjgs.144.3.0451

Castillo M, Torró L, Campeny M, Villanova C, Tauler E, Melgarejo JC (2009) Mineralogía del depósito de uranio Eureka (Castell-estaó, Pirineo, Catalunya). Macla, 11: 53–54

Chappaz A, Gobeil C, Tessier A (2010) Controls on uranium distribution in lake sediments. Geochimica et Cosmochimica Acta, 74: 203–214. doi: 10.1016/j.gca.2009.09.026

Church T (1994) Lithic ressources studies. A sourcebook for archaeologist. University of Tulsa, Tulsa

Conley DJ (2002) Terrestrial ecosystems and the global biogeochemical silica cycle. Global Biogeochemical Cycles 16: 1121. doi: 10.1029/2002GB001894

Costa E, Garcés M, López-Blanco M, Beamud E, Gómez-Paccard M, Larrasoaña JC (2010) Closing and continentalization of the South Pyrenean foreland basin (NE Spain): magnetochronological constraints. Basin Research 22: 904-917. doi: 10.1111/j.1365-2117.2009.00452.x

Costa E, Garcés M, Sáez A, Cabrera L, López-Blanco M (2011) The age of the "Grande Coupure" mammal turnover: new constraints from the Eocene–Oligocene record of the Eastern Ebro Basin (NE Spain). Palaeogeography, Palaeoclimatology, Palaeoecology 301: 97–107. doi: 10.1016/j.palaeo.2011.01.005

Del Santo G, García-Sansegundo J, Sarasa L, Torrebadella J (2000) Estratigrafía y estructura del Terciario en el sector oriental de la Cuenca del Ebro entre Solsona y Manresa (NE de España). Revista de la Sociedad Geologica de España 13: 265–278

Dunlop, D.J., Özdemir, Ö., 1997. Rock magnetism. Fundamentals and frontiers. Cambridge University Press, Cambridge

Feist M, Anadón P, Cabrera L, Choi SJ, Colombo F. Sáez A (1994) Upper Eocene–Lowermost Miocene charophyte succession in the Ebro Basin (Spain). Contribution to the charophyte biozonation in Western Europe. Newsletters on Stratigraphy 30: 1–32

Fuertes-Prieto MN, Neira-Campos A, Fernández-Martínez E, Gómez-Fernández F, Alonso-Herrero E (2014) Mucientes chert in the Northern Iberian Plateau (Spain). Journal of Lithic Studies 1: 117–135. doi: 10.2218/jls.v1i1.785

Gaspar-Escribano JM, Van Wees JD, Ter Voorde M, Cloetingh S, Roca E, Cabrera L, Muñoz JA, Ziegler PA, Garcia-Castellanos D (2001) Three-dimensional flexural modelling of the Ebro Basin (NE Iberia). Geophysical Journal International 145: 349–367

Götze J (2012) Classification, mineralogy and industrial potential of SiO_2 minerals and rocks. In Götze J, Möckel R (eds) Quartz: Deposits, Mineralogy and Analytics. Springer-Verlag, Berlin Heidelberg, pp 1–27

Götze J, Gaft M, Möckel R (2015) Uranium and uranyl luminescence in agate/chalcedony. Mineralogical Magazine 79: 985–995. doi: http://dx.doi.org/10.1180/minmag.2015.079.4.08

Graetsch HA, Grünberg JM (2012) Microstructure of flint and other chert raw materials. Archaeometry 54: 18–36. doi: 10.1111/j.1475-4754.2011.00610.x

Gromet PL, Dymek PF, Haskin LA, Korotev RL (1984) The "North American Shale Composite": its compilation, major and trace element characteristics. Geochimica et Cosmochimica Acta 48: 2469–2482. doi: 10.1016/0016-7037(84)90298-9

Heaney PJ, Post JE (1992) The Widespread Distribution of a Novel Silica Polymorph in Microcrystalline Quartz Varieties. Science, New Series 255: 441–443

Hesse R (1989) Silica diagenesis: origin of inorganic and replacement cherts. Earth-Science Reviews 26: 253–284. doi: 10.1016/0012-8252(89)90024-X

Inizan ML, Reduron M, Roche H, Tixier J (1995) Technologie de la pierre taillée. CNRS, Meudon

Jacka AD (1974) Replacement of fossils by length-slow chalcedony and associated dolomitization. Journal of Sedimentary Petrology 44: 421-427

Knauth LP (1979) A model for the origin of chert in limestone. Geology 7: 274–277. doi: 10.1130/0091-7613(1979)7<274:AMFTOO>2.0.CO;2

Knauth LP (1994) Petrogenesis of chert. Reviews in Mineralogy and Geochemistry 29: 233–258

Kruiver PP, Passier HF (2001) Coercivity analysis of magnetic phases in sapropel S1 related to variations in redox conditions, including an investigation of the S ratio. Geochemistry, Geophysics, Geosystems 2: 1–21. doi: 10.1029/2001GC000181

Lacombe S (2007) Aproximació petroarqueològica del sílex dels nivells azilians de la Balma de la Margineda. In Guilaine J, Barbaza M, Martzluff M (eds) Les excavaciones a la Balma de la Margineda (1979-1991), vol. IV. Gobern d'Andorra, Andorra, pp 540–573

Larrasoaña JC, Beamud E, Olivares M, Murelaga X, Tarriño A, Baceta JI, Etxebarria N (2016) Magnetic Properties of Cherts from the Basque-Cantabrian Basin and Surrounding Regions: Archaeological Implications. Frontiers in Earth Science 4: 1–8. doi: 10.3389/feart.2016.00035

Liu Q, Roberts AP, Larrasoaña JC, Banerjee SK, Guyodo Y, Tauxe L, Oldfiled F (2012) Environmental magnetism: Principles and applications. Reviews of Geophysics 50: 1–50. doi: 10.1029/2012RG000393

López-Martínez N, Arribas ME, Robador A, Vicens E, Ardèvol Ll (2006) Los carbonatos danienses de (Unidad 3) de la Fm Tremp (Pirineos Sur-Centrales): paleogeografía y relación con el límite Cretácico-Terciario. Revista de la Sociedad Geológica de España 19: 233–255

Loucaides S, Van Cappellen P, Behrends T (2008) Dissolution of biogenic silica from land to ocean: Role of salinity and pH. Limnology and Oceanography 53: 1614–1621

Lozano JA, Morgado A, Puga E, Martín-Algarra A (2010) Explotaciones del sílex tipo Turón (Málaga, España): localización y caracterización petrológica y geoquímica. Geogaceta 48: 163–166

Luedtke BE (1992) An Archaeologist's Guide to Chert and Flint. University of California, Los Angeles

Luzón A, González A (2000) Sedimentology and Evolution of a Paleogene-Neogene Shallow Carbonate Lacustrine System, Ebro Basin, Northeastern Spain. In Gierlowski-Kordesh EH, Kelts KR (eds) Lake Basins through Space and Time, APPG Studies in Geology 46. Boulder, Tulsa, pp 407–416

Luzón A, Rodríguez A (2003) Los sistemas aluviales Oligo-Miocenos del margen norte de la Cuenca del Ebro: caracterización sedimentaria y síntesis paleogeográfica. Revista de la Sociedad Geologica de España 16: 239–255

Macias I, Díaz M, Estrada R, Rampone G (1987) Facies de abanico fluvial en los afloramientos orientales de la Formación Peraltilla. Acta Geologica Hispanica 21-22: 19–26

Mangado X, Morales JI, Oms X, Rey M, Sánchez M (2012) Estudio de los restos líticos de la Cova Colomera (Prepirineo de Lleida) entre 5220 y 1660 cal BC. Análisis arqueopetrológico de las materias primas silíceas y posibles áreas de captación. In Borrell M et al (eds) Xarxes al Neolític. Circulació i intercanvi de matèries, productes i idees a la Mediterrània occidental. Museu de Gavà, Gavà, pp 155–161

Mangado X, Sánchez M, Bartrolí R, Tejero JM, Fullola JM, Avezuela B, Petit MA, Mercadal O (2014) Silex et coquillages. Approche à l'identification des territoires socio-économiques des Magdaleniens du Versant sud des Pyrenées catalans. In Otte M, Le Brun-Riscalens F (eds) Modes de contacts et de déplacements au Paléolithique eurasiatique. Université de Liège, Liège, pp 473–489

Mangado X, Sánchez M, Martínez-Grau H, González-Olivares C (in press) Prehistoric chert mining evidence in Serra Llarga (Castelló de Farfanya, Spain). Journal of Lithic Studies

Martin M (1974) Sobre la petrogenesis de algunas litofacies españolas con fases urano-orgánicas. Boletín Geológico y Minero 85: 561–581

Martínez J, Mora R (2009) Balma Guilanyà (Prepirineo de Lleida) y el Aziliense en el noreste de la Península Ibérica. Trabajos de Prehistoria 66: 45–60. doi: 10.3989/tp.2009.09021

Martínez J, de la Torre I, Mora R, Casanova J (2010) Technical variability and changes in the pattern of settlement at Roca dels Bous (Southeastern Pre-Pyrenees, Spain). In Conard NJ, Delagnes A (eds) Settlement dynamics of the Middle Paleolithic and Middle Stone Age. Kerns Verlag, Tübingen, pp 485–507

Mason B, Moore CB (1982) Principles of Geochemistry. Wiley, New York

Massey MS, Lezama-Pacheco JS, Nelson J, Fendorf S, Maher K (2014) Uranium Incorporation into Amorphous Silica. Environmental Science and Technology 48: 8636–8644. doi: 10.1021/es501064m

Matteson S, Avara MJ, Nguyen CV, Kim SH (2005) RBS characterization of uranium in flint and chert. Nuclear Instruments and Methods in Physics Research B 241: 465–469. doi: 10.1016/j.nimb.2005.07.057

Mazzucco N, Gassiot E, Ortega D, Clemente I, Rodríguez-Antón D (2013) Lithic procurement at the Cova del Sardo between the V-III Millennium cal BC: data on mobility strategies. Archeologia Postmedievale 17: 51–60

McBride EF, Abdel-Wahab A, El-Younsy ARM (1999) Origin of spheroidal chert nodules, Drunka Formation (Lower Eocene), Egypt. Sedimentology 46: 733–755. doi: 10.1046/j.1365-3091.1999.00253.x

Meece DE, Benninger LK (1993) The coprecipitation of Pu and other radionuclides with $CaCO_3$. Geochimica et Cosmochimica Acta 57: 1447–1458. doi: 10.1016/0016-7037(93)90005-H

Moh'd BK, Powell JH. (2010) Uranium distribution in the Upper Cretaceous-Tertiary Belqa Group, Yarmouk Valley, northwest Jordan. Jordan Journal of Earth and Environmental Sciences 3: 49–62

Morgado A, Lozano JA, Pelegrin J (2011) Las explotaciones prehistóricas del silex de la formación Milanos (Granada, España). Menga - Revista de Prehistoria de Andalucía 2: 135–155

Murray RW (1994) Chemical criteria to identify the depositional environment of chert: General principles and applications. Sedimentary Geology 90: 213–232. doi: 10.1016/0037-0738(94)90039-6

Odell GH (2004) Lithic Analysis. Kluwer Academic / Plenum Publishers, New York

Ortega D, Terradas X, Roqué C, Ibáñez J, Beamud E, Larrasoaña JC (2016) El sílex de la unidad de calizas de Montmaneu (sector oriental de la Cuenca del Ebro). Geogaceta 60

Ortí F (1990) Las formaciones evaporíticas del Terciario continental de la zona de contacto entre la Cuenca del Ebro y los Catalánides. In Ortí F, Salvany JM (eds) Formaciones evaporíticas de la Cuenca del Ebro y cadenas periféricas, y de la zona de Levante. ENRESA-Universidad de Barcelona, Barcelona, pp 133–154

Palomo A, Gibaja JF, Ortega D, Alonso N, Marín D, Moya A (2012) La industria lítica tallada del asentamiento de Minferri (Juneda, Lleida) a finales del III/primera mitad del II milenio cal. BC. Cypsela, revista de prehistòria i protohistòria 19: 103–122

Parcerisas J (1999) Análisis petroarqueológico de la Unidad UAS5 de la Cova de l'Estret de Tragó. In Pallí L, Roqué C (eds) Avances en el estudio del Cuaternario español. Universitat de Girona, Girona, pp 271–276

Pardo G (2004) La Cuenca del Ebro. In Vera JA (ed) Geología de España. Sociedad Geológica de España e Instituto Geológico y Minero de España, Madrid, pp 533–543

Piper DZ, Bau M (2013) Normalized Rare Earth Elements in Water, Sediments, and Wine: Identifyng Sources and Environmental Redox Conditions. American Journal of Analytical Chemistry 4: 69–83. doi: 10.4236/ajac.2013.410A1009

Rosell J, Linares R, Llompart C (2001) El Garumniense prepirenaico. Revista de la Sociedad Geologica de España 14: 47–56

Roy M, Tarriño A, Benito-Calvo A, Mora R, Martínez-Moreno J (2013) Aprovisionamiento de sílex en el Prepirineo oriental durante el Paleolítico superior antiguo: el nivel arqueológico 497C de Cova Gran (Santa Linya, Lleida). Trabajos de Prehistoria 70: 7–27. doi: 10.3989/tp.2013.00

Sáez A (1987) Estratigrafía y sedimentología de las formaciones lacustres del tránsito Eoceno-oligoceno del NE de la Cuenca del Ebro. PhD Thesis, Universidad de Barcelona

Sáez A, Anadón P, Herrero MH, Moscariello A (2007) Variable style of transition between Paleogene fluvial fan and lacustrine systems, southern Pyrenean foreland, NE Spain. Sedimentology 54: 367–390. doi: 10.1111/j.1365-3091.2006.00840.x

Sánchez M (2014) Detecting human mobility in the Pyrenees through the analysis of chert tools during the Upper Palaeolithic. Journal of Lithic Studies 1: 263-279. doi: 10.2218/jls.v1i1.778

Siever R (1962) Silica Solubility, 0º -200ºC., and the Diagenesis of Siliceous Sediments. The Journal of Geology 70: 127–150

Sturchio NC, Antonio MR, Soderholm L, Sutton SR, Brannon JC (1998) Tetravalent uranium in calcite. Science 281: 971-973. doi: 10.1126/science.281.5379.971

Tarriño A, Terradas X (2013) Materias primas líticas. In García-Diez M, Zapata L (eds) Métodos y técnicas de análisis y estudio en Arqueología prehistórica. De lo técnico a la reconstrucción de los grupos humanos. UPV/EHU, Vitoria-Gasteiz, pp 439–452

Tarriño A, Olivares M, Etxebarria N, Baceta JI, Larrasonaña JC, Yusta I, Pizarro JL, Cava A, Barandiarán I, Murelaga X (2007) El sílex de tipo Urbasa. Caracterización petrológica y geoquímica de un marcador litológico en yacimientos arqueológicos del Suroeste europeo durante el Pleistoceno superior y Holoceno inicial. Geogaceta 43: 127–130

Tarriño A, Duarte E, Santamaría D, Martínez L, Fernández J, Suárez P, Rodríguez V, Forcelledo E, de la Rasilla M (2013) El sílex de Piloña. Caracterización de una nueva fuente de materia prima lítica en la Prehistoria de Asturias. In de la Rasilla M (ed) Estudios en homenaje a FJ Fortea. Ediciones de la Universidad de Oviedo, Oviedo, pp 115–132

Tarriño A, Elorrieta I, García-Rojas M (2015) Flint as raw material in prehistoric times: Cantabrian Mountain and Western Pyrenees data. Quaternary international 364: 94–108. doi: 10.1016/j.quaint.2014.10.061

Taylor SR, McClennan SM (1985) The Continental Crustal: Its Composition and Evolution. Blacwell, Oxford

Terradas X (2001) La gestión de los recursos minerales en las sociedades cazadoras-recolectoras. CSIC, Barcelona

Terradas X (2012) Estudo do aprovisionamiento de matérias-primas de naturaleza mineral. In Gibaja JF, Carvalho AF (eds) Introdução ao estudo da pedra lascada. Edições Colibrí, Lisboa, pp 9–18

Terradas X, Ortega D, Boix J (2012) El projecte LITOCAT: creació d'una litoteca de referència sobre la disponibilitat de roques silícies a Catalunya. Tribuna d'Arqueologia, 2010-2011: 131–150

Terradas X, Ortega D, Marín D, Masclans A, Roqué C (in press) Neolithic flint quarries of Montvell (Catalan Pre-Pyrenees, Spain). In Pereira T, Bicho N, Terradas X (eds) Raw materials exploitation in Prehistory: Sourcing, processing and distribution. Cambrige Scholars Publishing

Thacker P, Ellwood B (2002) The magnetic susceptibility of cherts: Archaeological and geochemical implications of source variation. Geoarchaeology 17: 465–482. doi: 10.1002/gea.10023

Valero L, Garcés M, Cabrera L, Costa E, Sáez A (2014) 20 Myr of eccentricity paced lacustrine cycles in the Cenozoic Ebro Basin. Earth and Planetary Science Letters 408: 183–193. doi: 10.1016/j.epsl.2014.10.007

Wright P (1990) Lacustrine carbonates. In Tucker ME, Wright VP (eds) Carbonate sedimentology. Blackwell Science, Malden-Oxford, pp 164–190

Yang Y, Fang X, Li M, Galy A, Koutsodendris A, Zhang W (2015) Paleoenvironmental implications of uranium concentrations in lacustrine calcareous clastic-evaporite deposits in the western Qaidam Basin. Palaeogeography, Palaeoclimatology, Palaeoecology 417: 422–431. doi: 10.1016/j.palaeo.2014.10.002

Young RA (1993) The Rietveld method. International Union of Crystallography, Oxford

FIGURE CAPTIONS

Fig. 1a Map showing the main geological units of northeastern Iberia and the study area

Fig. 1b Detailed geological map showing central and western sectors of Castelltallat Formation (based on Sáez et al. 2007). The Montvell chert quarries and stratigraphic logs of figure 2 are located

Fig. 2 Detailed stratigraphic logs of the Castelltallat Formation in western and central sectors of Castelltallat Formation, based on Sáez (1987). Sampled localities (TC and CM) as well as Montvell chert quarries are pointed out on the columns. See map of figure 1B for locations

Fig. 3 Archaeological sites of NE Iberia where stone tools made of chert coming from the Castelltallat Formation have been identified (grey colour). Triangles: Lower-Middle Palaeolithic; Circles: Upper Palaeolithic - Mesolithic; Squares: Neolithic

1) Cova Alonsé; 2) Cueva del Moro de Olvena; 3) Espluga de Puyascada; 4) Abrigo de Forcas I; 5) Cueva de los Moros de Gabasa; 6) Cueva de Trocs; 7) Estret de Tragó; 8) Fuentes de San Cristobal; 9) Cova Colomera; 10) Abric Pizarro; 11) Montvell chert quarries; 12) Auvelles; 13) Balma de la Massana; 14) Forat de la Conqueta; 15) Cova Gran de Santa Linya; 16) Abric Vidal; 17) Roca dels Bous; 18) Muricecs; 19) Cova del Sardo; 20) Nerets; 21) Cova del Parco; 22) Cova de les Llenes; 23) Balma Margineda; 24) Camp del Colomer; 25) Balma de Guilanyà; 26) Montlleó; 27) Font del Ros

Fig. 4 Detail of the mode in which silicifications in the Castelltallat Formation occur. A and B, Tossal del Castell (Castelló de Farfanya, Serra Llarga); C and D, Cal Mestre (Calonge de Segarra, Serra de Castelltallat). The outline of the stratiform silicification is highlighted in C

Fig. 5 Macro- and microscopic details of the Castelltallat Formation chert. A) Chert with massive texture; B) Liesegang rings (hand samples from Algerri); C and D). Matrix of micro- and cryptocrystalline quartz and relict carbonates from the incrustation of stems of charophyte algae in a sample from Tossal del Castell. Note in D the cross-sections of charophyte internodes with different orientations. E) Chalcedony and megacrystalline granular quartz in the fill of the primary porosity of the rock. F) Ostracod shell replaced by lutecite (Lu) and fill in the

interior cavity of chalcedony (Cl) and megacrystalline quartz (Mq), in an identical sequential arrangement as in E. G-H) Opaque minerals (iron oxides?) (Op) and organic matter (Om) in a sample from Cal Mestre
Scale bar in A and B equivalent to 1cm, in E to 200μ, and to 500μ in the others. C, E. F and G photos were taken with crossed polars (XPL) and D and H with plane-polarised light (PPL)

Fig. 6 SEM images of the appearance of fresh fracture surfaces (A) and patinated surfaces (B) of the same chert from the Castelltallat Formation, from Algerri. The scale bar indicates 60μ in both images

Fig. 7 Rock magnetic data for the studied chert samples. A) Magnetic susceptibility (χ). Reference value for pure quartz is indicated as a dashed line. B) S- ratios vs IRM@1.2T for the studied samples. Whiskers indicate the interquartile ranges around the median values (large dots). C) χ plotted as a function of the log of the IRM@1.2T. All the studied samples fall in the range of diamagnetic chert

Fig. 8 Diagram with the NASC-normalised rare earths (REEs) results from the Castelltallat chert. See data in Table 3

TABLES

Sample	Quartz (%)	Calcite (%)	Moganite (%)	*L* (nm)
109CM	98.5	1.5	2.2	81.3
111CM	98.9	1.1	n.d.	76.9
112CM	99.1	0.9	n.d.	77.7
113CM	98.4	1.6	n.d.	74.0
114CM	98.9	1.1	n.d.	75.4
120CM	99.0	1.0	n.d.	83.7
39TC	92.3	1.7	6.0	68.3
40TC	89.7	5.3	5.0	77.0
42TC	94.2	n.d.	5.8	64.7
43TC	92.0	3.6	4.3	88.2
44TC	88.7	5.5	5.8	67.6

Table 1 Mineral composition of the chert based on XRD. The code identifying the samples corresponds to their inventory number in the LITOcat collection. TC: Tossal del Castell, CM: Cal Mestre. Percentages of the mineral composition are estimated regarding the sample volume; *L*: size of the quartz microcrystalline dominions obtained through Rietveld analysis

Chert locality	χ (10^{-9} kg/m^3)	IQR (10^{-10})	IRM@1.2T (10^{-6} Am^2/kg)	IQR (10^{-6})	S ratio	IQR	N
TC	-0.35	0.4	0.33	0.09	0.97	0.01	5
CM	-4.08	2.08	5.67	4.14	0.68	0.21	7

Table 2 Rock magnetic data for the chert from Castelltallat Fm; IQR: InterQuartile Range

		370TC	371TC	372TC	358CM	359CM	360CM	361CM
Major elements (%)	SiO_2	93,80	94,00	97,40	94,40	91,30	83,80	87,20
	CaO	0,25	1,46	0,72	2,81	4,19	7,91	3,52
	Fe_2O_3	2,69	0,85	1,06	0,56	0,54	0,22	1,44
	Al_2O_3	0,28	0,24	0,34	0,30	0,14	0,15	0,38
	MgO	0,06	0,08	0,07	0,08	0,07	0,12	0,10
	Na_2O	0,05	0,04	0,07	0,08	0,07	0,06	0,11
	K_2O	0,04	0,04	0,05	0,08	0,04	0,04	0,10
	TiO_2	0,01	0,01	0,02	0,02	0,01	0,01	0,02
	MnO	0,03	0,01	0,01	0,01	0,01	0,01	0,02
	P_2O_5	<0.01	0,01	<0.01	<0.01	0,02	<0.01	0,02
	SrO	<0.01	0,01	<0.01	0,01	0,01	0,02	0,01
	BaO	0,02	0,02	0,01	<0.01	<0.01	<0.01	<0.01
Trace elements (ppm)	Ba	155,50	178,50	116,00	20,70	12,40	17,20	25,80
	Co	2,00	1,00	1,00	1,00	1,00	<1	1,00
	Cs	0,11	0,08	0,10	0,10	0,03	0,03	0,11
	Ga	3,00	1,50	1,60	1,60	2,00	1,40	1,50
	Hf	0,20	0,40	2,90	0,30	0,20	0,20	0,30
	Nb	1,50	0,70	0,50	0,50	0,40	0,30	1,10
	Rb	2,40	1,50	2,20	2,00	0,70	0,70	2,50
	Sn	1	<1	1	<1	<1	<1	<1
	Sr	22,70	64,50	31,40	66,50	84,20	153,00	81,40
	Ta	0,1	0,1	0,1	<0.1	<0.1	<0.1	<0.1
	Th	0,35	0,26	0,37	0,30	0,11	0,14	0,32
	U	4,13	2,84	5,34	64,50	51,40	59,80	51,60
	V	6,00	6,00	6,00	5,00	<5	<5	6,00
	W	1,00	1,00	1,00	<1	<1	<1	<1
	Zr	6,00	14,00	115,00	9,00	5,00	3,00	10,00
	Mo	<1	1,00	<1	29,00	2,00	2,00	3,00
	Cu	49,00	12,00	9,00	26,00	3,00	7,00	26,00
	Pb	6,00	2,00	5,00	4,00	<2	3,00	3,00
	Zn	39,00	20,00	32,00	5,00	2,00	5,00	4,00
	Ni	2,00	1,00	1,00	1,00	<1	<1	2,00
	As	12,20	6,40	6,00	8,40	2,90	3,20	7,60
	Cd	<0.5	<0.5	<0.5	<0.5	<0.5	<0.5	<0.5
	Sb	1,13	0,47	0,50	1,32	0,52	0,51	1,22
	Bi	0,35	0,15	0,16	0,03	0,02	0,02	0,04
	Ag	<0.5	<0.5	<0.5	0,90	0,50	0,60	0,90
	Hg	0,05	0,01	0,03	0,01	0,01	0,01	0,01
	Se	0,20	<0,2	<0,2	<0,2	<0,2	<0,2	<0,2
	Cr	<0.01	<0.01	<0.01	<0.01	<0.01	<0.01	<0.01
	Y	0,70	0,60	0,90	0,70	<0.5	0,50	0,90
LOI (%)		0,70	1,99	1,69	3,15	4,27	6,59	4,43
Total C (%)		0,17	0,46	0,29	0,71	0,99	1,80	0,88
Total S (%)		0,08	0,05	0,05	0,02	0,03	0,04	0,04

Table 3 Geochemical composition (major and trace elements) of the analysed samples

	r		*r*
SiO_2	-0.628	**Rb**	-0.374
CaO	0.773 *	**Sr**	0.706
Fe_2O_3	-0.577	**Th**	-0.532
Al_2O_3	-0.248	**V**	-0.725
MgO	0.592	**Zr**	-0.478
Na_2O	0.588	**Cu**	-0.234
K_2O	0.588	**Pb**	-0.325
TiO_2	0.205	**Zn**	-0.902 **
MnO	-0.318	**Ni**	0.067
Ba	-0.959 **	**As**	-0.409
Co	-0.440	**Sb**	0.297
Cs	-0.409	**Bi**	-0.833 *
Ga	-0.404	**Ag**	0.321
Hf	-0.465	**Hg**	-0.691
Nb	-0.441	**LOI**	0.820 *

Table 4 Bilateral correlation coefficients (Pearson's r) for U with a selection of major and trace components in chert from the Castelltallat Fm. * statistically significant correlation for p>0.05; **, very significant for p>0.01

	La	Ce	Pr	Nd	Sm	Eu	Gd	Tb	Dy	Ho	Er	Tm	Yb	Lu	ΣREE	Ce/Ce*	Eu/Eu*	La_n/Yb_n	La_n/Ce_n
NASC*	31.10	66.70	7.70	27.40	5.59	1.18	4.90	0.85	4.17	1.02	2.84	0.48	3.06	0.46	157.45	1	1	1	1
370TC	1.00	1.70	0.20	0.80	0.16	< 0.03	0.14	0.02	0.11	0.02	0.09	0.01	0.06	0.01	4.32	0.88	-	1.64	1.26
371TC	1.30	1.50	0.17	0.60	0.13	< 0.03	0.12	0.02	0.12	0.02	0.06	0.01	0.05	0.01	4.11	0.74	-	2.56	1.86
372TC	1.30	1.90	0.22	0.90	0.16	0.03	0.14	0.02	0.16	0.03	0.11	0.02	0.12	0.02	5.13	0.82	0.89	1.07	1.47
358CM	1.00	1.60	0.20	0.70	0.12	< 0.03	0.14	0.02	0.10	0.02	0.06	0.01	0.07	0.01	4.05	0.83	-	1.41	1.34
359CM	0.60	0.80	0.08	0.30	0.06	< 0.03	0.07	0.01	0.05	0.01	0.03	< 0.01	0.04	< 0.01	2.05	0.85	-	1.48	1.61
360CM	0.70	0.90	0.11	0.40	0.08	< 0.03	0.09	0.01	0.08	0.01	0.05	< 0.01	0.04	< 0.01	2.47	0.75	-	1.72	1.67
361CM	1.20	1.90	0.23	0.80	0.15	0.03	0.17	0.02	0.13	0.03	0.09	0.01	0.07	0.01	4.84	0.84	0.83	1.69	1.35
Media	0.98	1.40	0.16	0.60	0.12	0.03	0.12	0.02	0.10	0.02	0.06	0.01	0.06	0.01	3.67	0.82	0.86	1.60	1.50

Table 5 Rare earths (REEs) content in the analysed chert samples

Figure 1a

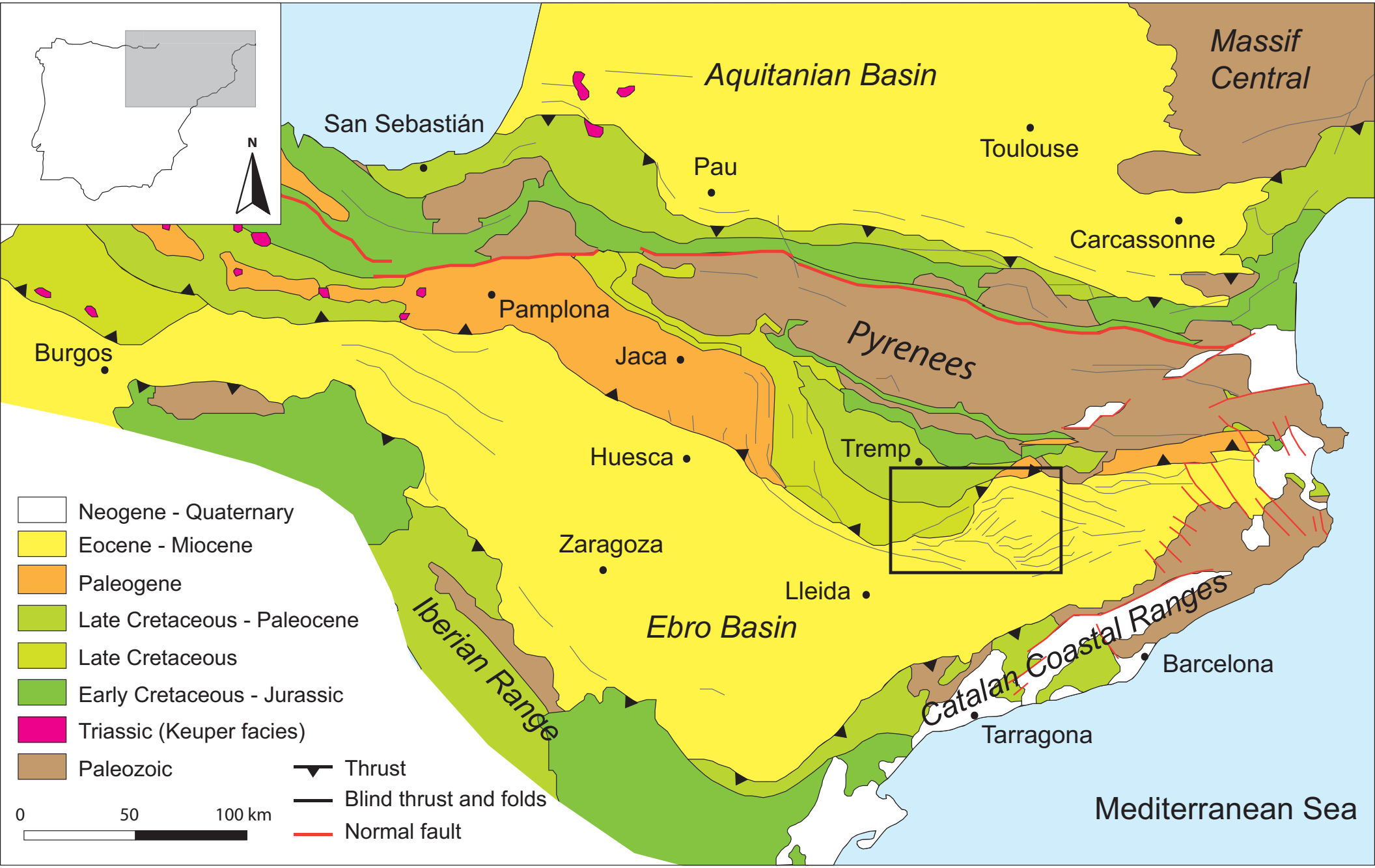
Aquitanian Basin
Massif Central
San Sebastián
Toulouse
Pau
Carcassonne
Pamplona
Pyrenees
Burgos
Jaca
Tremp
Huesca
Zaragoza
Lleida
Ebro Basin
Iberian Range
Catalan Coastal Ranges
Barcelona
Tarragona
Mediterranean Sea
N
Neogene - Quaternary
Eocene - Miocene
Paleogene
Late Cretaceous - Paleocene
Late Cretaceous
Early Cretaceous - Jurassic
Triassic (Keuper facies)
Paleozoic
Thrust
Blind thrust and folds
Normal fault
0
50
100 km

Figure 1b

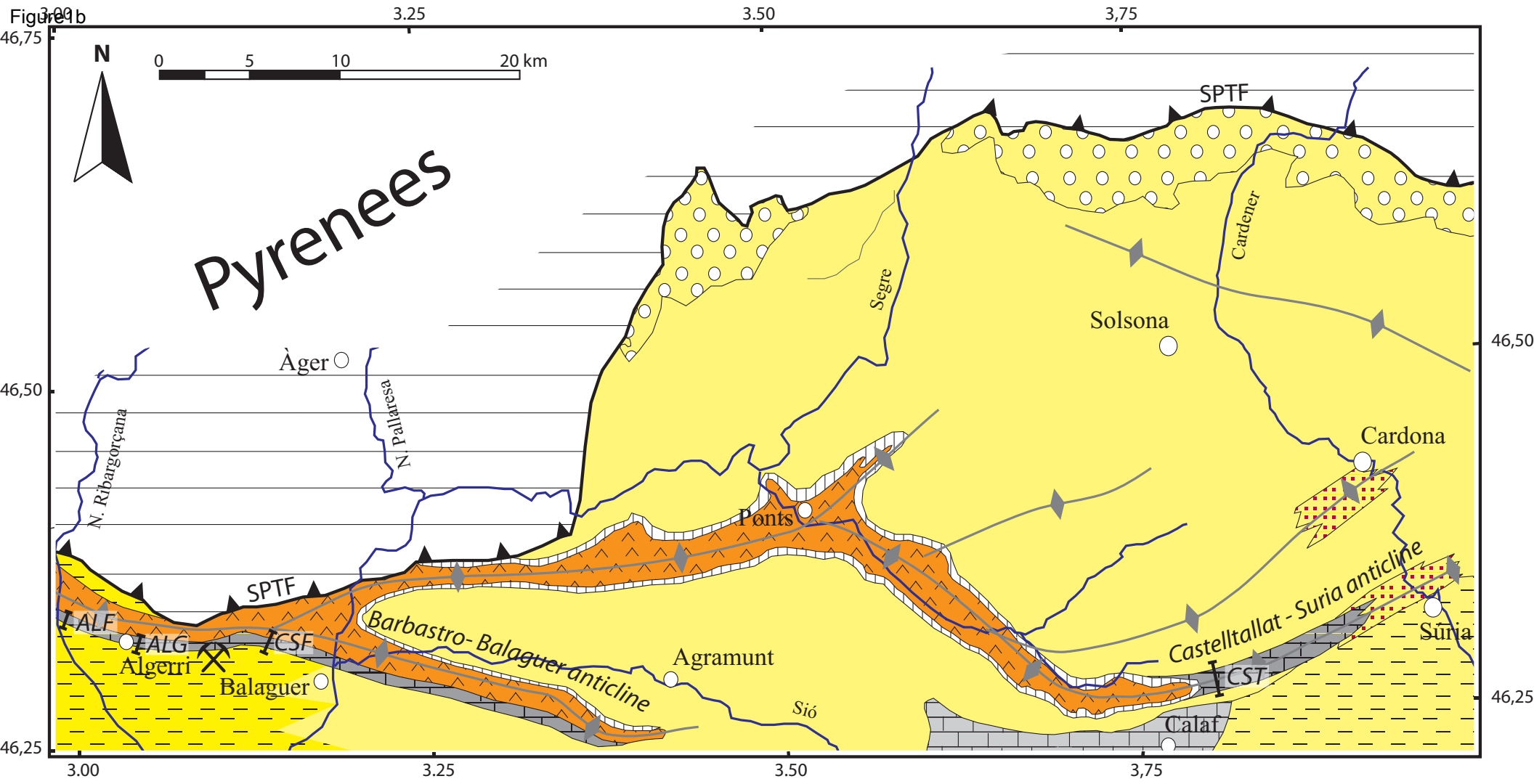

PYRENEES (Mesozoic - Paleocene)

PYRENEAN ALLUVIAL COMPLEX

- Conglomerates (Berga Group)
- Sandstones, red mudstones (Solsona Fm)
- Sandstones, mudstones (Suria Fm)
- Sandstones, red mudstones (Peraltilla Fm)

CATALAN COASTAL RANGE ALLUVIAL COMPLEX

- Sandstones, mudstones (Artés Fm)

LA NOGUERA LACUSTRINE SYSTEM

- Limestones, marly limestones, mudstones (Castelltallat Fm)
- Carbonated siltstones, sandstones, limestones (Torà Fm)
- Gypsum (Barbastro Fm)

LA SEGARRA LACUSTRINE SYSTEM

- Limestones, marls, coal (Calaf Fm)

- Anticline
- Thrust

SPTF South Pyrenean Thrust Front

Montvell chert quarries

Stratigraphic logs

Figure 2

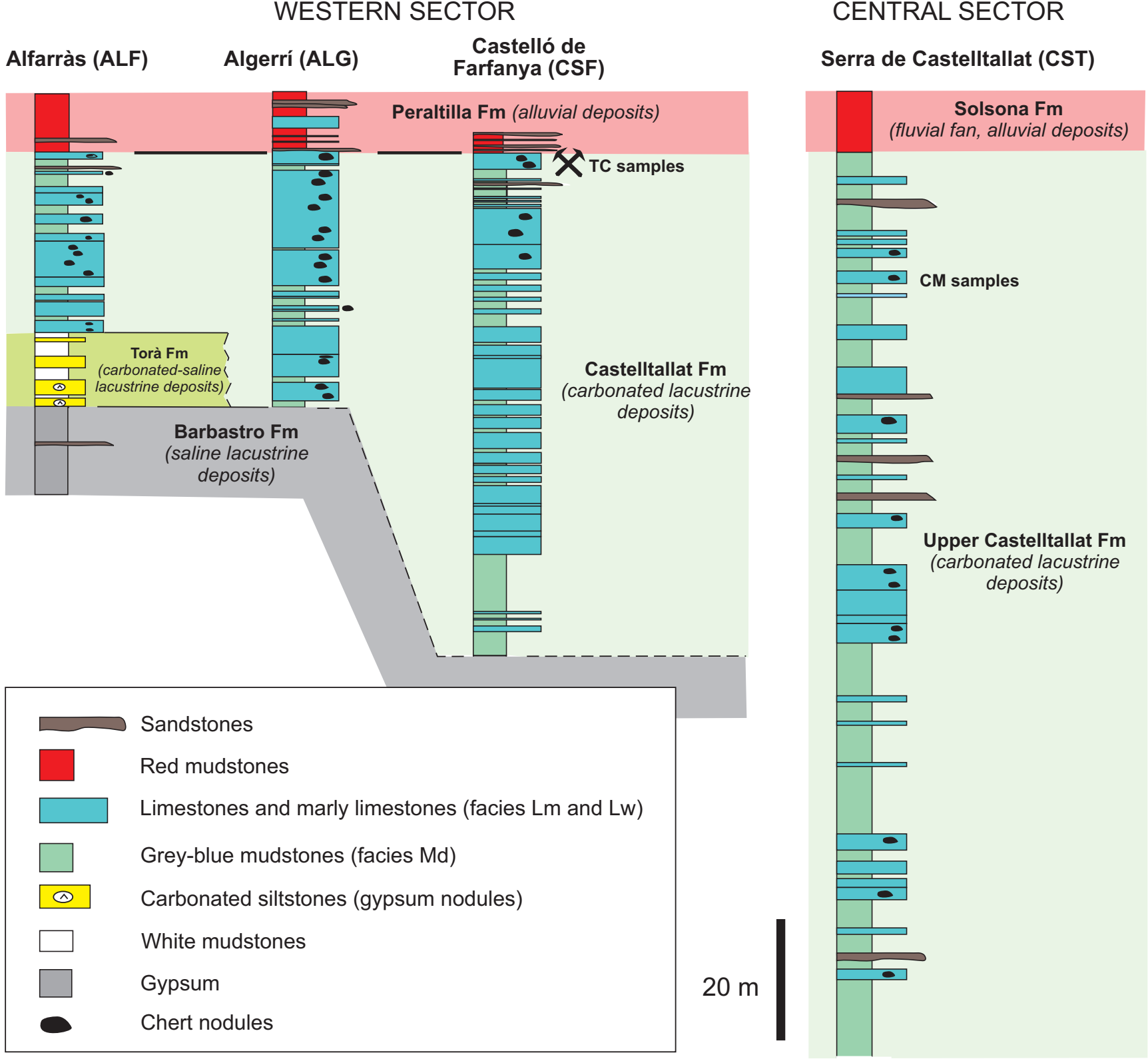
WESTERN SECTOR
CENTRAL SECTOR
Alfarràs (ALF)
Algerrí (ALG)
Castelló de Farfanya (CSF)
Serra de Castelltallat (CST)
Peraltilla Fm (alluvial deposits)
TC samples
Torà Fm (carbonated-saline lacustrine deposits)
Barbastro Fm (saline lacustrine deposits)
Castelltallat Fm (carbonated lacustrine deposits)
Solsona Fm (fluvial fan, alluvial deposits)
CM samples
Upper Castelltallat Fm (carbonated lacustrine deposits)
Sandstones
Red mudstones
Limestones and marly limestones (facies Lm and Lw)
Grey-blue mudstones (facies Md)
Carbonated siltstones (gypsum nodules)
White mudstones
Gypsum
Chert nodules
20 m

Figure 3

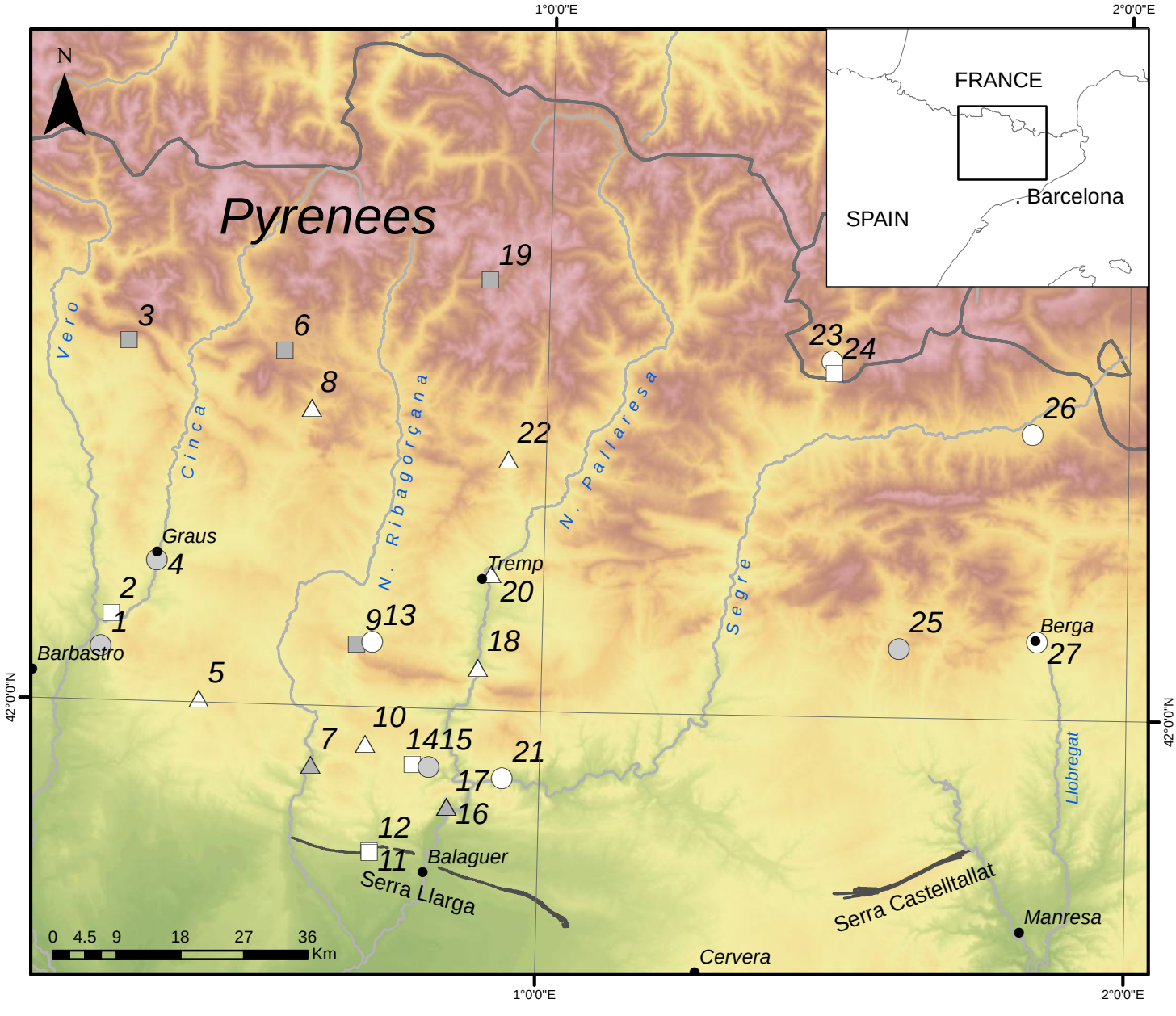
1°0'0"E
2°0'0"E
42°0'0"N
N
Pyrenees
FRANCE
SPAIN
Barcelona
Vero
Cinca
N. Ribagorçana
N. Pallaresa
Segre
Llobregat
Graus
Tremp
Barbastro
Berga
Balaguer
Serra Llarga
Serra Castelltallat
Manresa
Cervera
1
2
3
4
5
6
7
8
9
10
11
12
13
14
15
16
17
18
19
20
21
22
23
24
25
26
27
0 4.5 9 18 27 36
Km

Figure 4

Click here to download Figure Fig4.tif

Figure 5

Click here to download Figure Fig5.tif

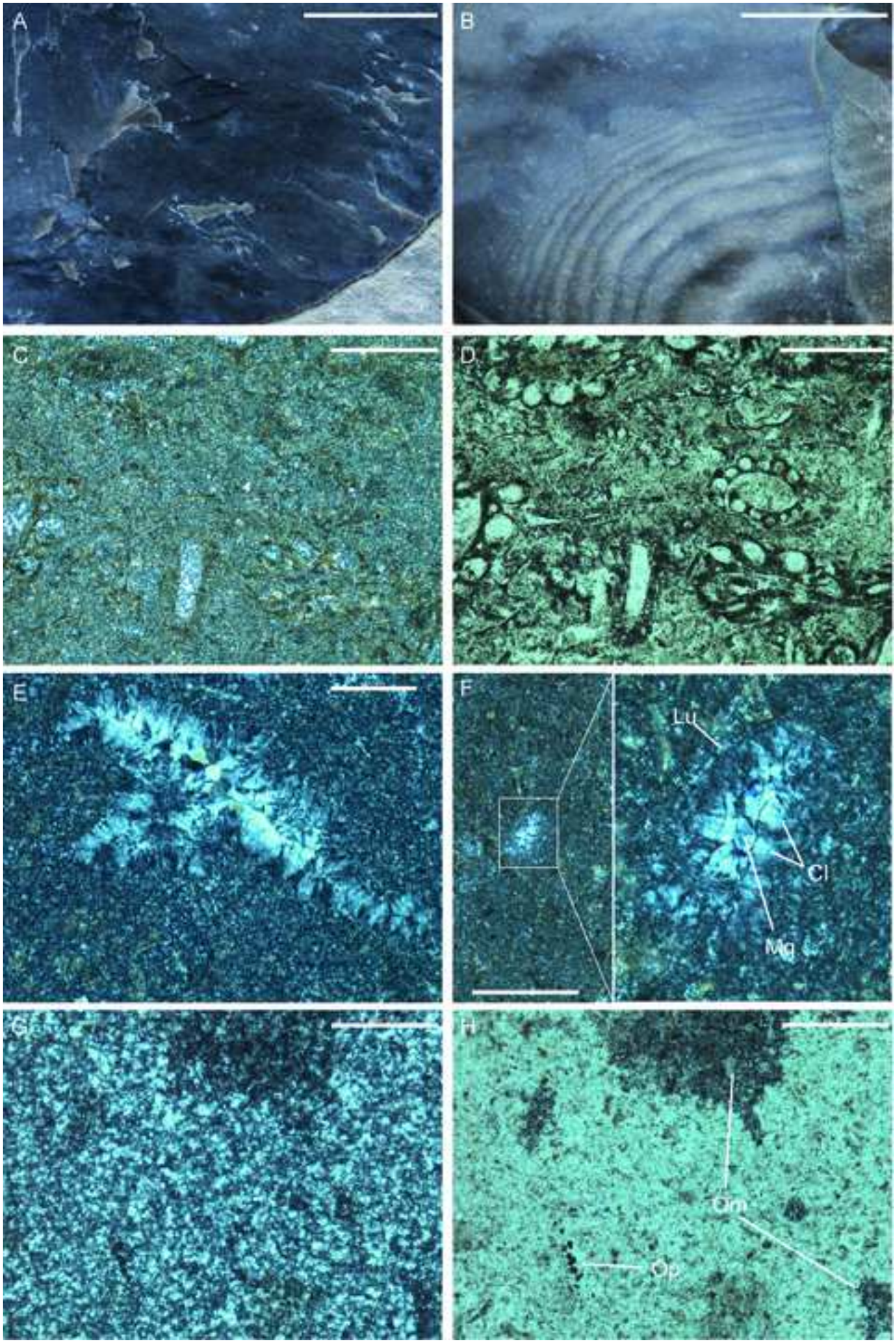

Figure 6

Click here to download Figure Fig6.tif

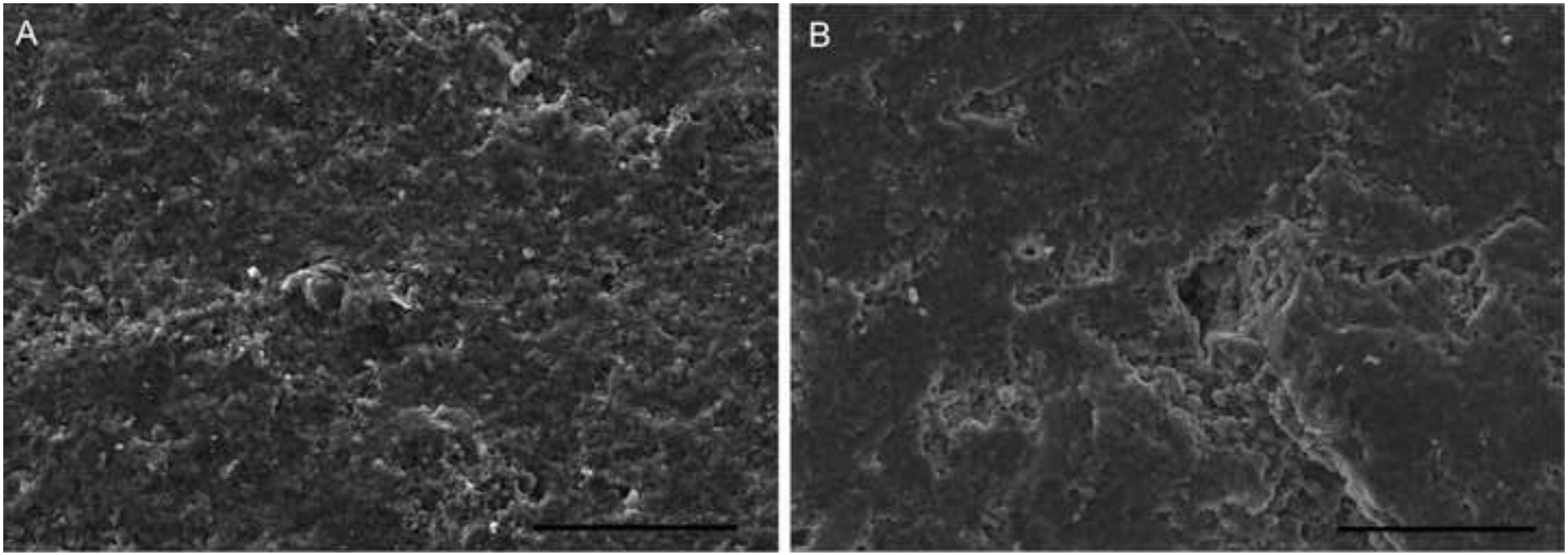

Figure 7

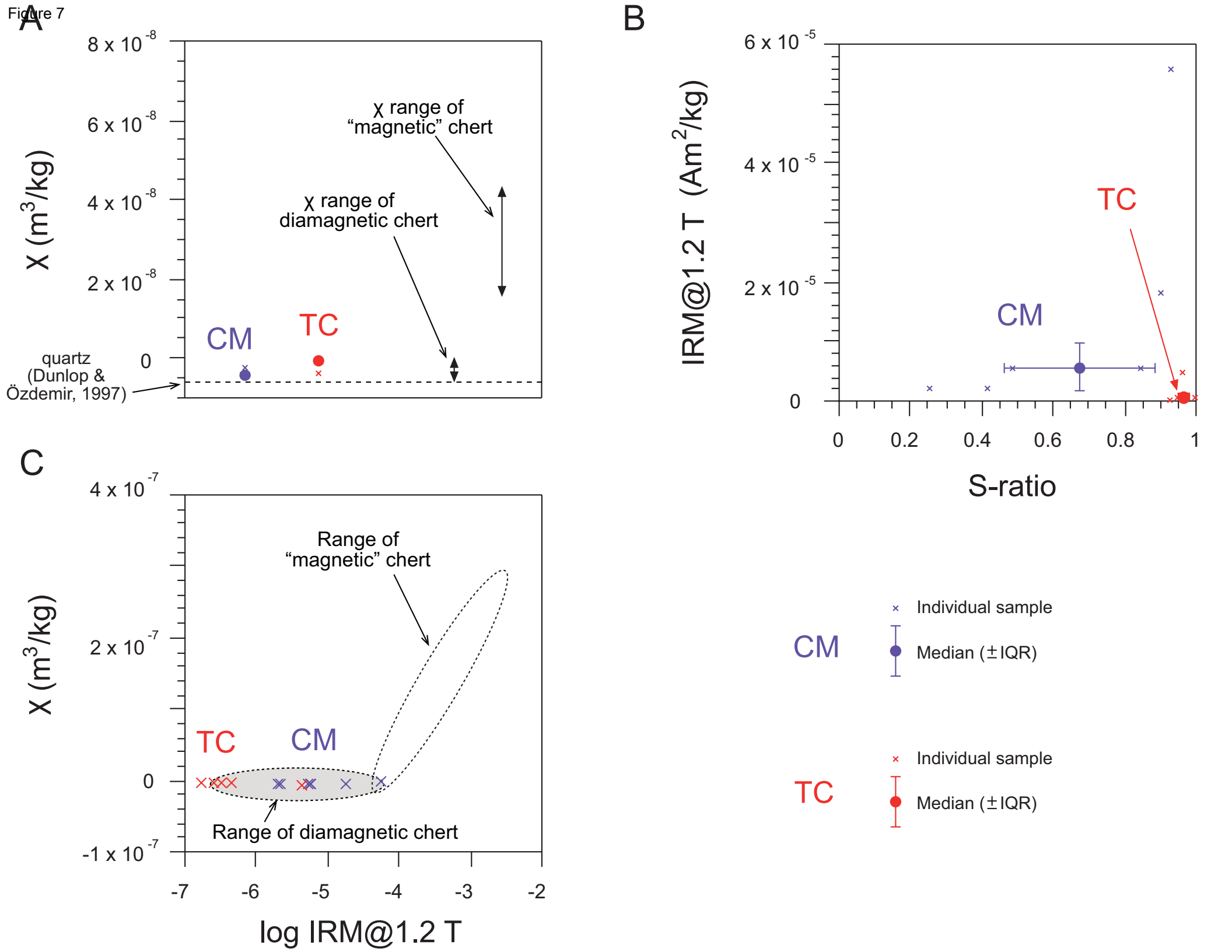
A
8 x 10 -8
6 x 10 -8
4 x 10 -8
2 x 10 -8
0
χ (m3/kg)
χ range of "magnetic" chert
χ range of diamagnetic chert
CM
TC
quartz (Dunlop & Özdemir, 1997)
B
6 x 10 -5
4 x 10 -5
2 x 10 -5
0
IRM@1.2 T (Am2/kg)
TC
CM
0
0.2
0.4
0.6
0.8
1
S-ratio
C
4 x 10 -7
2 x 10 -7
0
-1 x 10 -7
χ (m3/kg)
Range of "magnetic" chert
TC
CM
Range of diamagnetic chert
-7
-6
-5
-4
-3
-2
log IRM@1.2 T
CM
Individual sample
Median (±IQR)
TC
Individual sample
Median (±IQR)

Figure 8

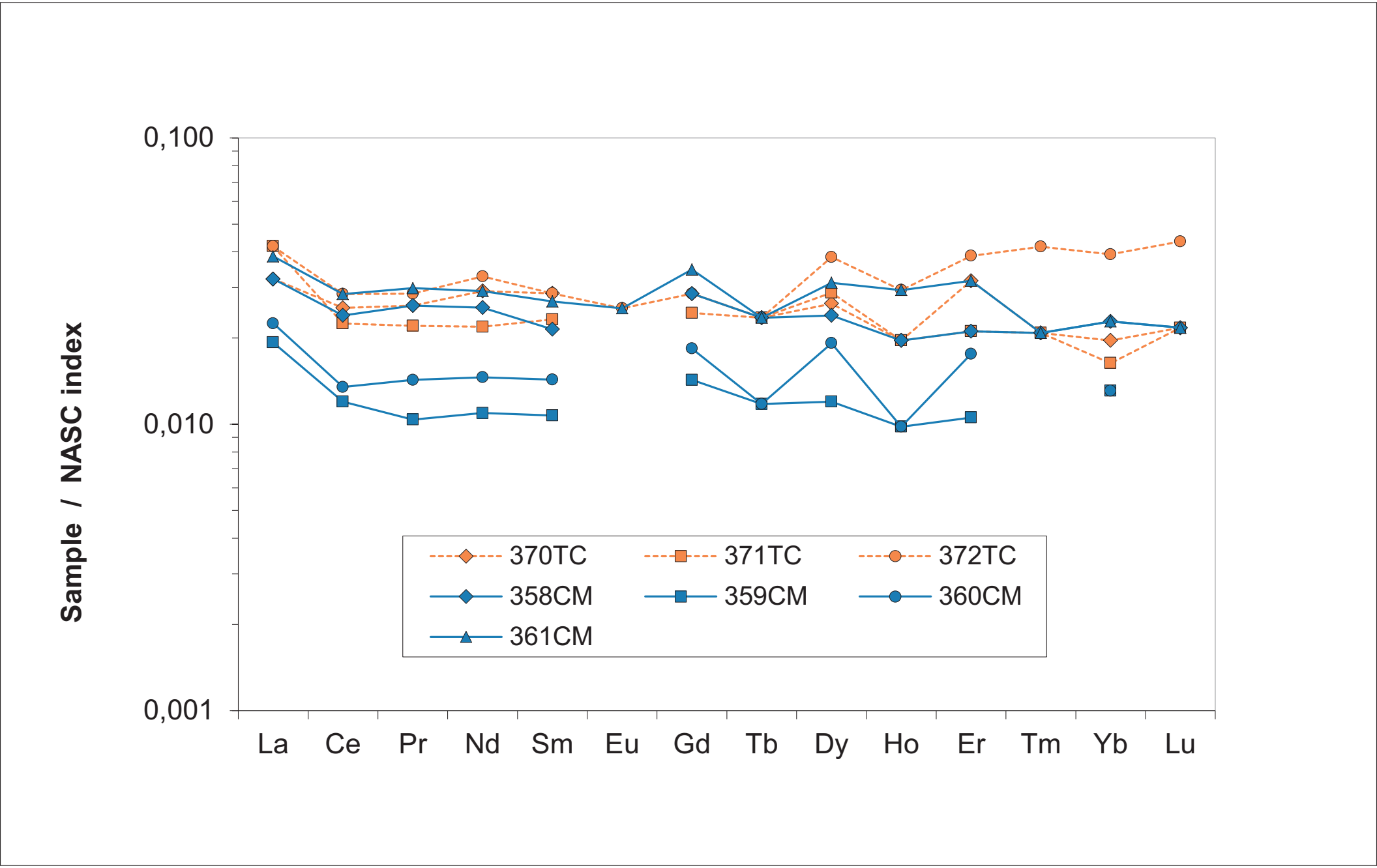
0,100
0,010
0,001
Sample / NASC index
La
Ce
Pr
Nd
Sm
Eu
Gd
Tb
Dy
Ho
Er
Tm
Yb
Lu
370TC
371TC
372TC
358CM
359CM
360CM
361CM